A STUDY OF HORIZONTAL CELL - PHOTORECEPTOR INTERACTION IN THE FROG RETINA USING A RANDOMLY MODULATED STIMULUS

Thesis by

Ronald Benjamin Melton

In Partial Fulfillment of the Requirements

for the Degree of

Doctor of Philosophy

California Institute of Technology

Pasadena, California

1981

(Submitted August 20, 1980)

AKNOWLEDGEMENTS

I would like to thank my wife, Carol Geier, for her love and support during my tenure as a graduate student. I probably could have done it without her, but it wouldn't have been as pleasant.

I would also like to thank my advisor, Dr. G. D. McCann, and several other faculty members including Dr. Derek Fender and Dr. T. K. Caughey for their support and guidance. I would like to thank Dr. Mark Citron for teaching me the techniques necessary to perform experiments on the frog eyecup and for his continual encouragement. I would also like to thank him for his comments on this thesis. I would like to thank Dr. John Kroeker for his comments as well and for a new perspective on white noise analysis. I would like to thank Dr. Tom Ogden and the members of his lab at Estelle Doheney Eye Foundation for assistance in preparing tissue for light microscopy, Mr. Ron Fargason for explaining the term perikarya and other mysterious things to me and all of the staff of the Bioinformation Systems department at Caltech for kindness and assitance when needed. Last, but not least, I would like to thank Dr. William R. Levick for his encouragement and advice. His boundless energy was an inspiration to me and his experimental expertise was very helpful when I needed to improve my results. I also thank the Fairchild Scholars Program for bringing him to Caltech.

This work was supported in part by a National Research Service Award (1 T32 GM07737) from the National Institute of General Medical Science.

Abstract

The intracellular responses of frog horizontal cells and photoreceptors to conventional and randomly modulated stimuli were recorded by intracellular probing using glass micropipettes. The stimuli were designed to test for photoreceptor response compression by surround illumination. The results indicated that the response of photoreceptors is reduced by stimulation of the area surrounding the cell's receptive field. It appeared that the effect is generated by negative feedback from horizontal cells to both rods and cones. These findings are in good agreement with the results of earlier studies by other investigators who established that horizontal cells feed back to cone photoreceptors in many vertebrate species.

Table of Contents

1. INTRODUCTION

Our visual system is one of our more complex senses. It collects and processes information about our surroundings at a phenomenal rate providing us with a three dimensional picture of the world around us. In the retina the information is collected and processing is begun. In this initial stage of processing the collection system is adapted to the level of illumination of the surroundings. The retinal neurons also begin to process the visual image, passing on signals to the brain where the picture we 'see' is developed.

The retina is actually a specialized part of the brain unlike the other senses which develop from the embryonic neural crest. During development of a vertebrate embryo outgrowths of the forebrain appear and grow out until they come in contact with the epidermis. The outgrowths then invert and develop into the optic cup while the epidermis develops into the lens [3].

The fully developed retina has five major types of neurons. Figure 1-1 illustrates the general organization of the five elements. At the outermost layer of the retina are the photoreceptors. Here the light is collected and transduced into an electrical signal. This signal is transferred from the photoreceptors to the horizontal cells and bipolar cells. The horizontal cells spread the signal spatially in the outer layer of the retina while the bipolar cells transmit the signal on to

the rest of the system. The amacrine cells and ganglion cells receive the signal from the bipolar cells. The amacrine cells spread the signal spatially in the inner layer of the retina and provide further input to the ganglion cells. The ganglion cells are the final processing stage of the retina. They integrate the information they receive from the bipolar and amacrine cells and transmit the resulting signal on to the brain and other parts of the central nervous system.

The system is, of course, not as simple as I have described. In the frog retina in particular there are four types of photoreceptors, at least two types of horizontal and bipolar cells and several types of amacrine and ganglion cells [23]. There are also interactions between some of the cells which make the system even more complicated.

The outer plexiform layer, where the horizontal cells and photoreceptors are located, is a particularly interesting place to study these interactions. All of the cells in this layer of the retina respond to stimuli with graded potentials, that is slow continuous changes in their membrane potential [91]. In contrast to this most neurons respond to stimulation by generating fast voltage spikes. It is thought, however, that sometimes these spikes result from the neuron integrating graded potentials from other cells. Because the cells in the outer plexiform layer respond only with graded potentials studies of this part of the retina may provide information about how cells throughout the nervous system integrate the signals

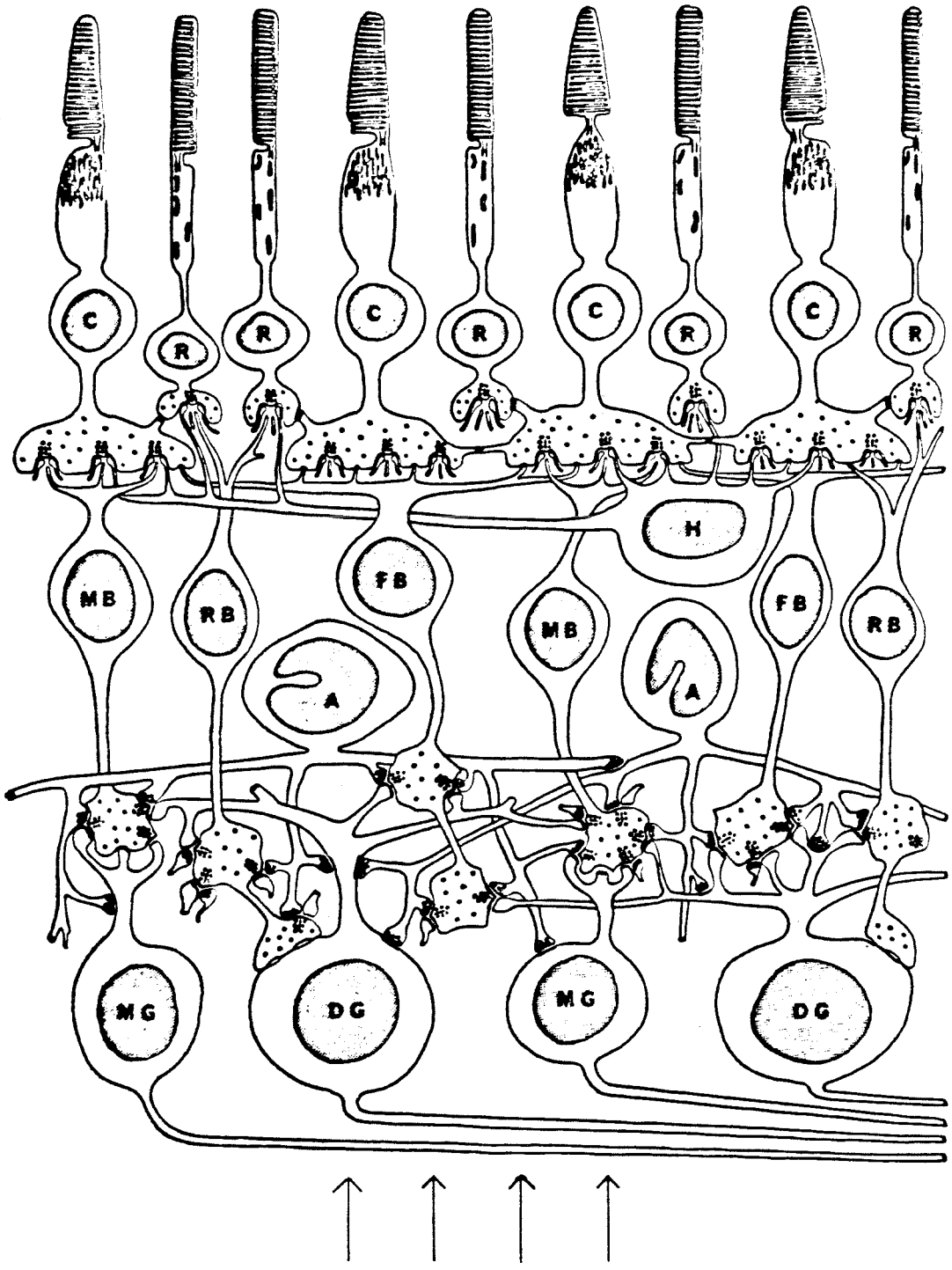

Figure 1-1 Organization of the vertebrate retina. R: Rod photoreceptor C: Cone photoreceptor H: Horizontal cell MB,RB and FB: Bipolar cells A: Amacrine cell MG and DG: Ganglion cells. From Dowling and Boycott (1966).

from other neurons. In studying the vertebrate visual system researchers have traditionally tested the system using stimuli such as annuli and spots whose intensities are pulsed between dark and light. The resulting impulse response of the system has then been used as evidence for various hypotheses about how the visual system works. This type of stimulus is not, however, a natural one for the visual system. It is so harsh that it may put the system in a state it would never be in in day to day use.

Under normal operating conditions our visual system sees a random set of patterns over any appreciable amount of time. By looking up from this page and looking around the room your visual system will encounter countless objects whose images are uncorrelated with one another. Because the system encounters a random set of stimuli under normal operating conditions it makes sense to study the system by stimulating it with random inputs. Besides being 'natural' a random stimulus also exhaustively tests the system. In a long enough experiment a random stimulus will present all possible combinations of inputs to the system in an objective manner. Several researchers have recently begun to use this approach to study biological systems with great success [45,53,54,57,70].

This dissertation presents the results of a study of interactions between photoreceptors and horizontal cells in the outer plexiform layer of the retina of the frog Rana pipiens. The study was performed using a combination of traditional and

randomly modulated stimuli. These stimuli were designed to test the hypothesis that horizontal cells pool information about the average illumination on large areas of the retina and feed this information back to the photoreceptors thereby altering the sensitivity of the photoreceptors to light. The second chapter briefly summarizes the results of earlier investigations in the outer plexiform layer of the vertebrate retina. The third chapter describes the experimental and analytical techniques used in this study. The analytical section develops the set of orthogonal functionals for a randomly modulated uniformly distributed N-level stimulus. The fourth chapter presents the results of this study and the fifth chapter discusses these results and how they relate to the studies described in the second chapter.

2. BACKGROUND

2.1 GENERAL

There are five types of neurons in the vertebrate retina. They are the photoreceptors, horizontal cells, bipolar cells, amacrine cells and ganglion cells. Figure 2-1 illustrates the results of an examination of the structure and synaptic organization of the frog retina [23]. The cells are basically segregated into layers. The outer nuclear layer contains the receptor nuclei. The inner nuclear layer contains the horizontal, bipolar, and amacrine cell nuclei. The final layer, the ganglionic layer, contains the ganglion cell nuclei.

The synaptic areas are also segregated into two plexiform layers. The photoreceptors, horizontal cells and bipolar cells synapse in the outer plexiform layer. The bipolar, amacrine and ganglion cells synapse in the inner plexiform layer. This study is concerned with the outer plexiform layer of the frog retina.

In the frog retina there are four types of photoreceptors: red and green rods and single and double cones. The basic difference in the rods and cones, apart from having different photopigments, is in the shape of the outer segment. This shape difference was used in descriptively naming the two elements. The rods have long cylindrical outer segments and the cones have a short conical outer segment. The rod outer segment is about 2.0 times longer than that of the cone [21,23].

The double cone has two parts, one that is the same as a single cone and the other which is embryologically related to the red rods. The double cones seem to form when single cones and red rods come in close contact during early development. The two neurons become attached to each other and the rod takes on some of the structural characteristics of a cone [21].

The inner segments of the photoreceptors are very similar. They end in the outer plexiform layer with the receptor terminals. The receptor terminals of rods and cones are basically the same in the frog retina [23,29]. These terminals are the sites where synapses are formed between the photoreceptors and the horizontal and bipolar cells.

As can be seen in figure 2-1 the horizontal cells lie just proximal to the photoreceptors. In the frog retina there are two types of horizontal cells, the inner, or internal and the outer, or external. The inner cells are characterized by a large cell body with a small dendritic field and a single axon. The cell bodies are in close contact with each other almost like a layer of bricks. The external horizontal cells are characterized by small cell bodies, large dendritic fields and a single axon. Though their cell bodies are not in close contact, like the inner cells, their dendritic fields are tightly woven forming a feltlike layer. These close contacts within the two layers of horizontal cells are thought to explain their receptive field properties.These properties will be discussed in a later section. There are no apparent contacts between the two layers of horizontal cells [23].

The horizontal cells send their dendrites to the photoreceptor terminals where along with the bipolar cells they form synapses with the photoreceptors. In the retinas of fishes and primates it has been found that the horizontal cell and bipolar cell processes form triads where they contact the receptor terminals [23,25,60,77,79]. The triads have a bipolar cell process in the center with a horizontal cell process on either side. This arrangement is thought to hold for all vertebrate retinas.

There are several types of synapses formed at the receptor terminals. The horizontal cell-bipolar cell triads invaginate the receptor terminals and a ribbon synapse is formed between the receptors and the higher order neurons. More conventional synapses are also formed between the various elements. There is evidence that receptors are coupled via gap junctions with each other and with processes of flat bipolar cells. There is also evidence in goldfish of synapses from horizontal cells back to cones [23,25,77,79].

The bipolar cell nuclei are located proximal to the horizontal cell layers. They send their axons to the inner plexiform layer where they form synapses with the amacrine and ganglion cells. The bipolar cell is the only proven link between the two synaptic layers of the retina.

The amacrine and ganglion cells integrate the information supplied by the bipolar cells. The ganglion cell axons come together and form the optic nerve which carries information about

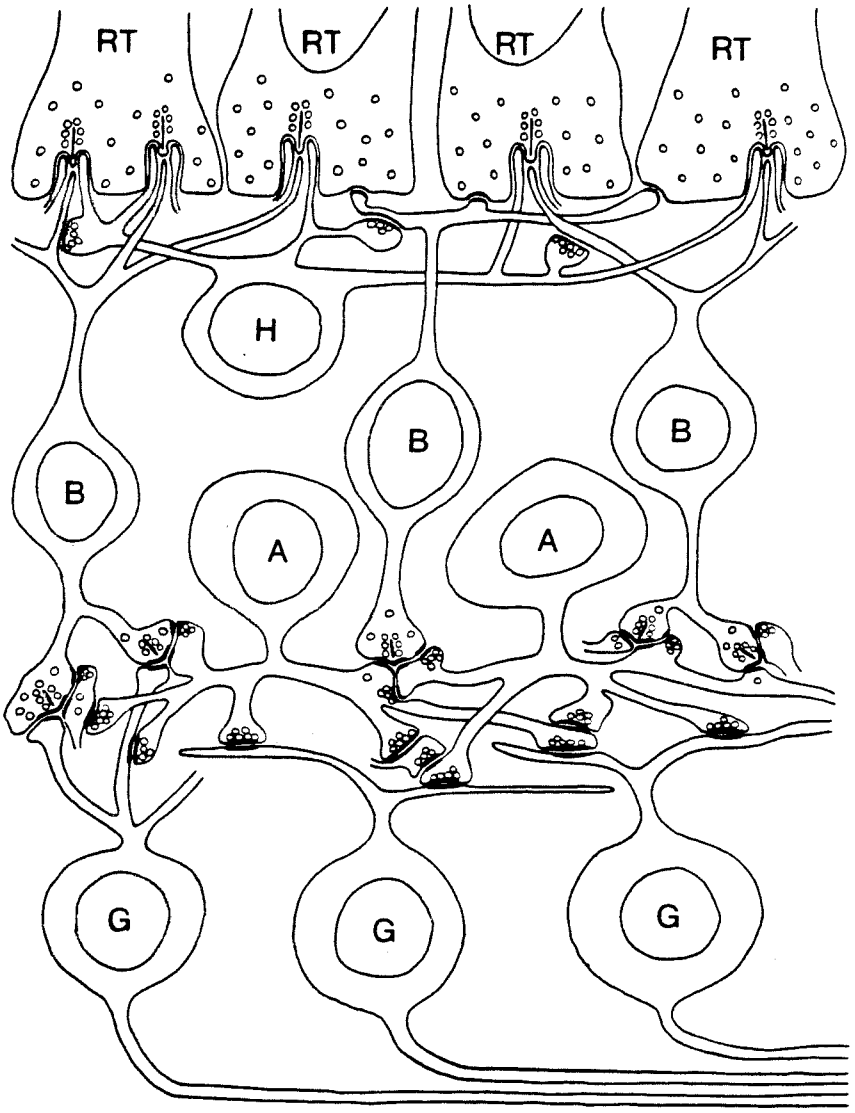

Figure 2-1 Organization of the frog retina. Receptor terminals: RT Horizontal cell: H Bipolar cell: B Amacrine cell: A Ganglion cell: G. From Dowling (1968).

the retinal image on to the the central nervous system.

2.2 ELECTROPHYSIOLOGY

The basic electrophysiological properties of the rods, cones and horizontal cells are very similar. The first part of this section will discuss these basic properties and the succeeding parts will deal with the particular properties of each element.

Unlike most neurons the three of interest here are depolarized under resting conditions. In the darkness they have a resting membrane potential of about 30 mV. This compares to a resting membrane potential of about 60 mV for most neurons [82,85,86]. They are also unusual in the way they respond to stimulation. In general neurons respond to stimulation with transient spikes of their membrane potential. These spikes are then carried along axons, the cables of the nervous system, to other neurons. The responses of ganglion cells and amacrine cells as shown in figure 2-2 illustrate a typical spike response. This figure also shows the type of response typical of photoreceptors and horizontal cells. In contrast to the spike response, these cells respond to flashes of light with slow hyperpolarizing changes in membrane potential. Notice that the horizontal cell responds to stimulation over a larger area than the photoreceptor. Notice also that the horizontal cell has a slower response than the photoreceptor. For the responses shown in figure 2-2 the horizontal cell response peaks about 500 milliseconds after the photoreceptor peaks.

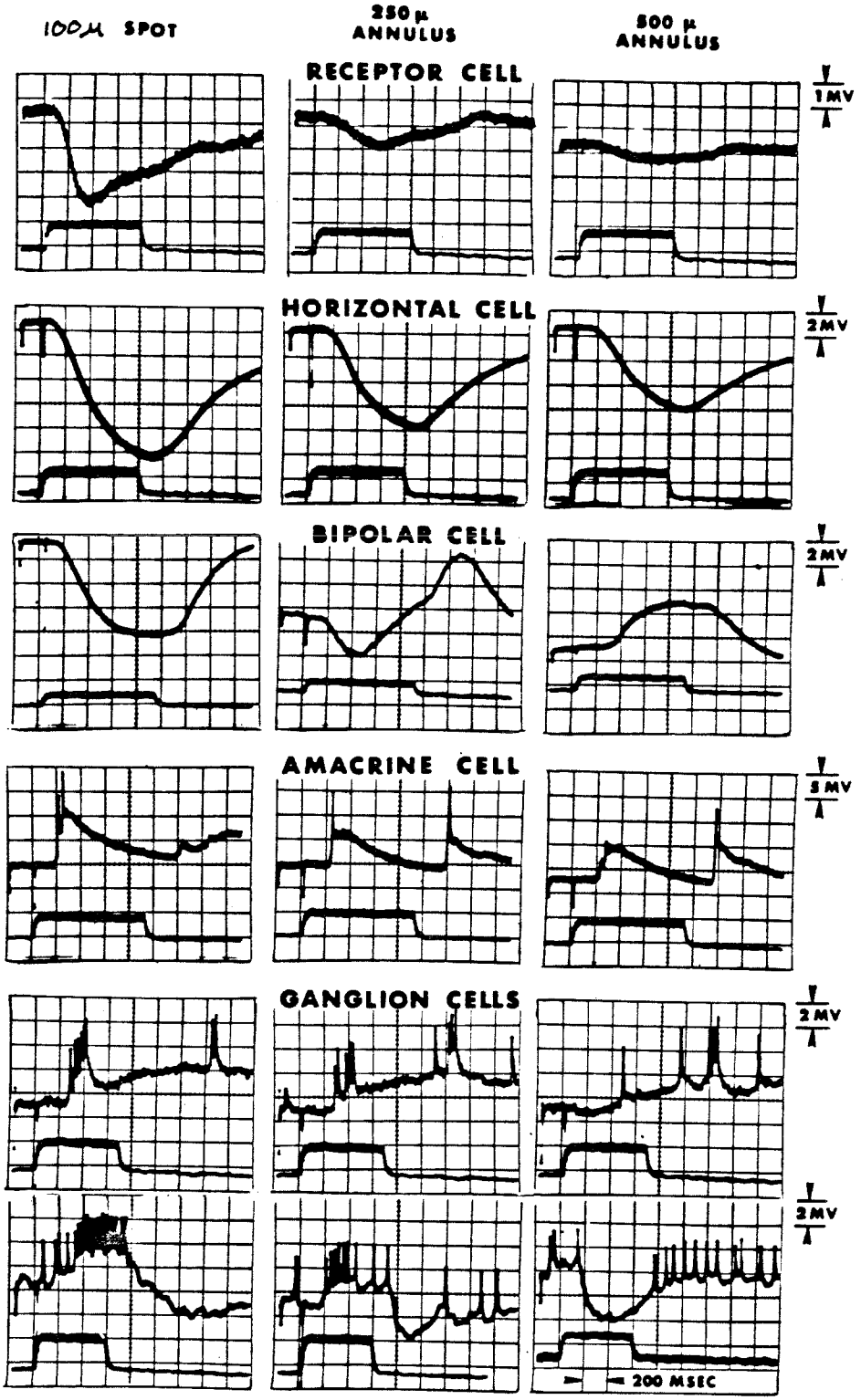

Figure 2-2 Intracellular recordings from neurons in the mudpuppy retina. The stimuli used were a spot of light focused on the electrode (left) and a small and large annulus (center and right). From Werblin and Dowling (1969).

2.2.1 Horizontal Cells

Electrophysiological studies of horizontal cells have been carried out in several species. The most commonly studied ones are the fishes [41,42,62-64], turtles [76,33,34,42], and amphibians [50,51,58,80]. Though there are morphological differences between the retinas of the various species there is strong consistency in the electrophysiology of horizontal cells.

Electrophysiologically, horizontal cells are classified as L-type or C-type, L standing for luminosity and C for chromaticity. L-type cells have a hyperpolarizing response to light of all wavelengths. C-type cells, on the other hand, respond to some wavelengths with hyperpolarization and to others with depolarization.

It is well known that functionally defined horizontal cell receptive fields are much larger than their dendritic fields. In the frog retina, for example, horizontal cell dendritic fields range from 15 to 40 microns in diameter while their receptive fields are between 300 and 1100 microns in diameter [59,70]. This dramatic ratio in field sizes has been accounted for by models which view the horizontal cells as a layer of resistive material through which signals may spread laterally. Marmarelis and Naka (1972), for example, approximated the horizontal cell layer in catfish as a continuous and homogeneous layer of resistive material bounded on top and bottom by a membrane of much higher resistance. Simon (1973) proposed a resistor network to model the

receptive fields of L1 and L2 horizontal cells in the turtle retina.

These resistive models are based on morphological evidence of gap junctions in some species and on physiological evidence of tight electrical coupling in others. For instance, in the dogfish retina studies have shown that intracellular polarization of one horizontal cell can give rise to polarization in a neighboring cell of the same layer separated by as many as five cells [42]. Recent studies in the carp retina have also shown electrical coupling between horizontal cells of the same type [84].

There is no direct evidence for the existence of gap junctions between horizontal cells in the frog retina; however, based on their large receptive field to dendritic field ratio and on the close contact between adjacent cells within the layers, coupling is probably electrotonic in nature.

The tight coupling of horizontal cells has led to hypotheses that horizontal cells pool information relating to a) average light intensity in large regions, b) chromatic inputs in the retina and c) that the pooling of information is used in mediation of bipolar cell receptive field surround. Thibos and Werblin (1978) showed that the sensitivity of the bipolar cell receptive field center is affected by steady illumination of the bipolar cell receptive field surround. Their experiments did not show what level of the retina was involved in the center surround interaction. Thibos and Werblin explained the result with direct

horizontal cell input to the bipolar cell. It is just as possible that the horizontal cells could be adjusting the sensitivity of the photoreceptors making up the bipolar cell receptive field center. Horizontal cell to photoreceptor feedback has also been proposed as the mechanism for generation of bipolar cell surround responses in the carp retina [84].

In fact there is strong support from other studies for such a hypothesis. Although there have not been any studies that directly assess the possibility of horizontal cell involvement with gain control at the photoreceptor level there have been several studies on horizontal cell feedback to photoreceptors for other reasons. There have been studies in the turtle retina showing that chromatically coded feedback exists (Cervetto and Fuortes, 1978). This chromatically coded feedback is thought to explain the existence of C-type responses in horizontal cells. These results have led to models such as the one shown in figure 2-3.

One study by Baylor, Fuortes and O'Bryan (1971) clearly demonstrated feedback from horizontal cells to cones in the retina of the turtle. They found that if bright steady illumination was centered over a cone photoreceptor then a bright flash in the surrounding area caused a depolarization of the photoreceptor. They also made simultaneous recordings from cones and L-type horizontal cells. The results of these recordings also support the contention that there is negative feedback from horizontal cells to cones. Finally, they conclusively demonstrated a feedback path by

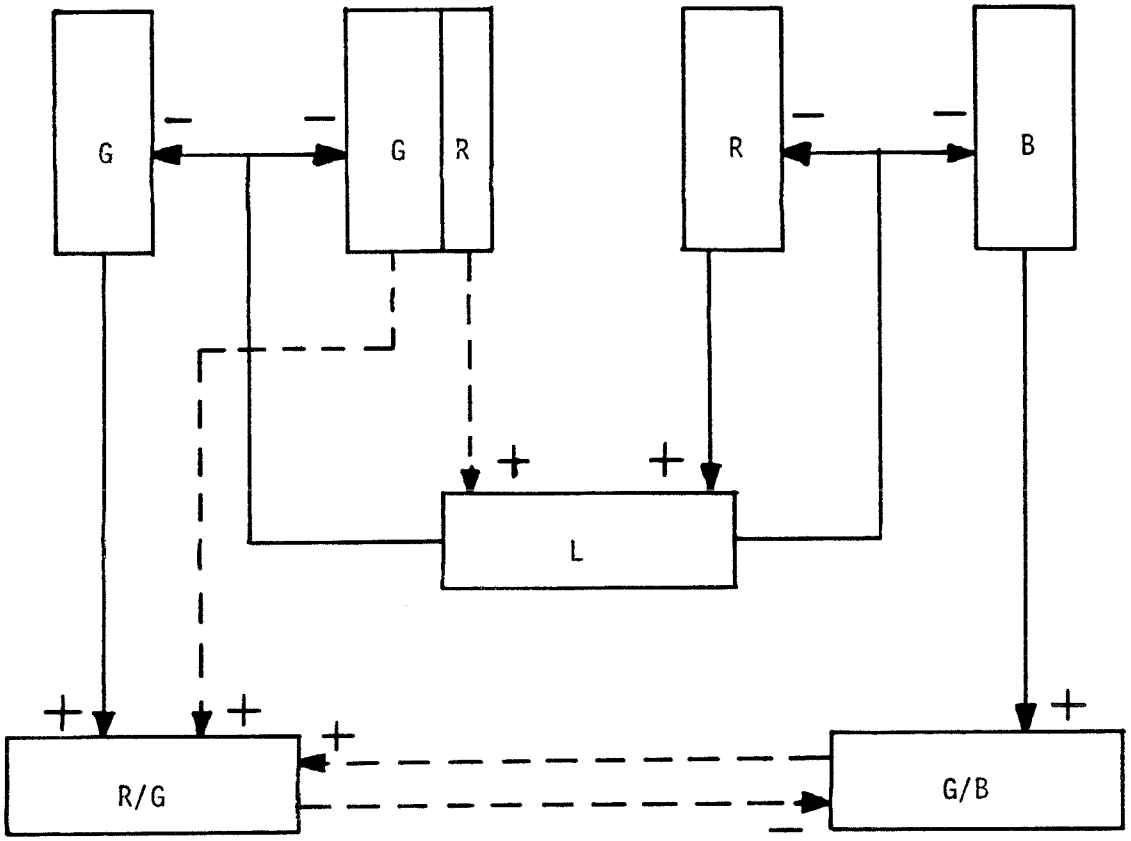

Figure 2-3 Proposed connections between horizontal cells and photoreceptors to generate C-type horizontal cell responses in the turtle retina. Solid lines are main connections and dashed lines are accesory interactions. + and - denote transmission with or without inversion of polarity. G: green cones; R: red cones; B: blue cones; adjoining GR cones represent double cones. L: Luminosity type horizontal cell and R/G and G/B chromaticity horizontal cells.
From Fuortes and Simon (1974).

polarizing cones by injecting current into nearby horizontal cells.

2.2.2 Photoreceptors

Due to the technical difficulty there have been few recordings from photoreceptors in the frog retina. The only known intracellular recordings of photoreceptors in the frog are from the rods in the retina of the bullfrog, Rana caesbeiana [83]. There have been, however, many reports of intracellular recordings from rods in the retina of the sea toad, Bufo marinus [13,30,31,36] and from rods and cones in the retina of the turtle [5-9,15,16,18-20,65-69,73-75]. From these studies it is known that relatively speaking rods have a slow response to the onset of a flash of light with no off response and a slow recovery to the membrane resting potential. Cones, on the other hand, have a fast response to both the onset and offset of a flash of light.

Since most of the results described above are for particular spatial patterns of retinal illumination it is important to consider the receptive field properties of the photoreceptors. At one time it was thought that the response recorded from individual photoreceptors was not influenced by the neighboring photoreceptors. Recent studies have shown, however, that photoreceptors do not respond independently but are strongly influenced by neighboring photoreceptors.

In the turtle retina studies have been done on the coupling of cones [6] and on the coupling of rods [13,15,16,73-75]. There

have also been studies on the coupling of rods in the retina of the sea toad, Bufo marinus, [30,31,36] and in the tiger salamander [89]. In the tiger salamander receptive field measurements indicate a diameter of 8 to 10 rods, approximately 120–150 microns, implying that each rod is coupled to about 80 neighbors. Studies in the retina of the sea toad agree well with this. Several independent studies have found rod receptive fields in the sea toad to be 100 to 150 microns in radius [36,68].

One study of cones in the turtle retina showed that some neighboring cones are electrically coupled at distances less than 40 microns [6]. This implies that cone receptive fields are from 40 to 100 microns in radius.

Studies have shown that much of the sensitivity change produced by changes in average illumination of the retina takes place at the photoreceptor level [10,7,26,30,43,65,69]. Two types of sensitivity change have been described. One of these is due to a static nonlinearity [7,8] between light intensity and membrane potential. This sensitivity change is also referred to as response compression [10]. The other type of sensitivity change is seen as a shift of the intensity response curve along the intensity axis and is referred to as cellular adaptation[65].

Response compression allows the system to have a response which is almost linear with respect to intensity over a range of about 1.5 log units of intensity. Cellular adaptation allows the almost linear region of response compression to center itself to

an average level of illumination that may span about 10 log units of intensity.

2.2.3 Bipolar cells Though the studies mentioned above have shown that most adaptation takes place at the level of the individual photoreceptor, another form of adaptation has been demonstrated as well. As was previously mentioned Thibos and Werblin (1978) showed that illumination of the surround of a bipolar cell receptive field altered the sensitivity of the center of the receptive field to light. This study implies that horizontal cells are involved in this adaptation because of the large amount of retinal area covered by the bipolar cell surround.

Other bipolar cell studies have also implied that horizontal cells mediate the bipolar cell surround [52,84]. One of the studies showed that current injection in nearby horizontal cells could polarize bipolar cells [52].

Though the results of these studies have implied a pathway from horizontal cells to bipolar cells they have not shown whether the path is direct or indirect. The results of these studies combined with the results of studies demonstrating negative feedback from horizontal cells to cone photoreceptors led to the hypothesis for the studies described in chapter four. The hypothesis is that photoreceptor sensitivity to light should be altered by illumination of the area surrounding the photoreceptor's receptive field.

3. MATERIALS AND METHODS

3.1 EXPERIMENTAL

An eyecup preparation of the frog, R. pipiens, was used for all experiments. The eye was removed and cut in half with a razor blade. The vitreous was then removed by placing strips of tissue paper around the eyecup. After draining the vitreous, the the eyecup was placed in a special holder on filter paper saturated with frog ringers. A small annulus of tissue paper was placed on the retina to mark the area recorded from after processing.

The retina was maintained in a moist environment of 100% oxygen at room temperature. Glass micropipettes with impedances of 100 - 200 megohms were used. These pipettes were filled with 2% horseradish peroxidase (HRP) in 0.2 molar potassium chloride (KCl). The micropipettes were advanced through the retina in 4 micron steps using a Burleigh 'Inchworm' micromanipulator. Plate 3-1 is a photograph of the recording station. After recording HRP was sometimes injected into the neuron by passing 5 nanoamp current pulses through the electrode for 10 seconds.

If an injection was made the retina was left undisturbed for 5 to 10 minutes to allow the HRP to diffuse throughout the injected neuron. The section of retina marked by the paper annulus was then dissected out and fixed for one hour in 1.5% gluteraldehyde. It was then washed overnight in a sodium phosphate buffer. At a later time it was reacted with

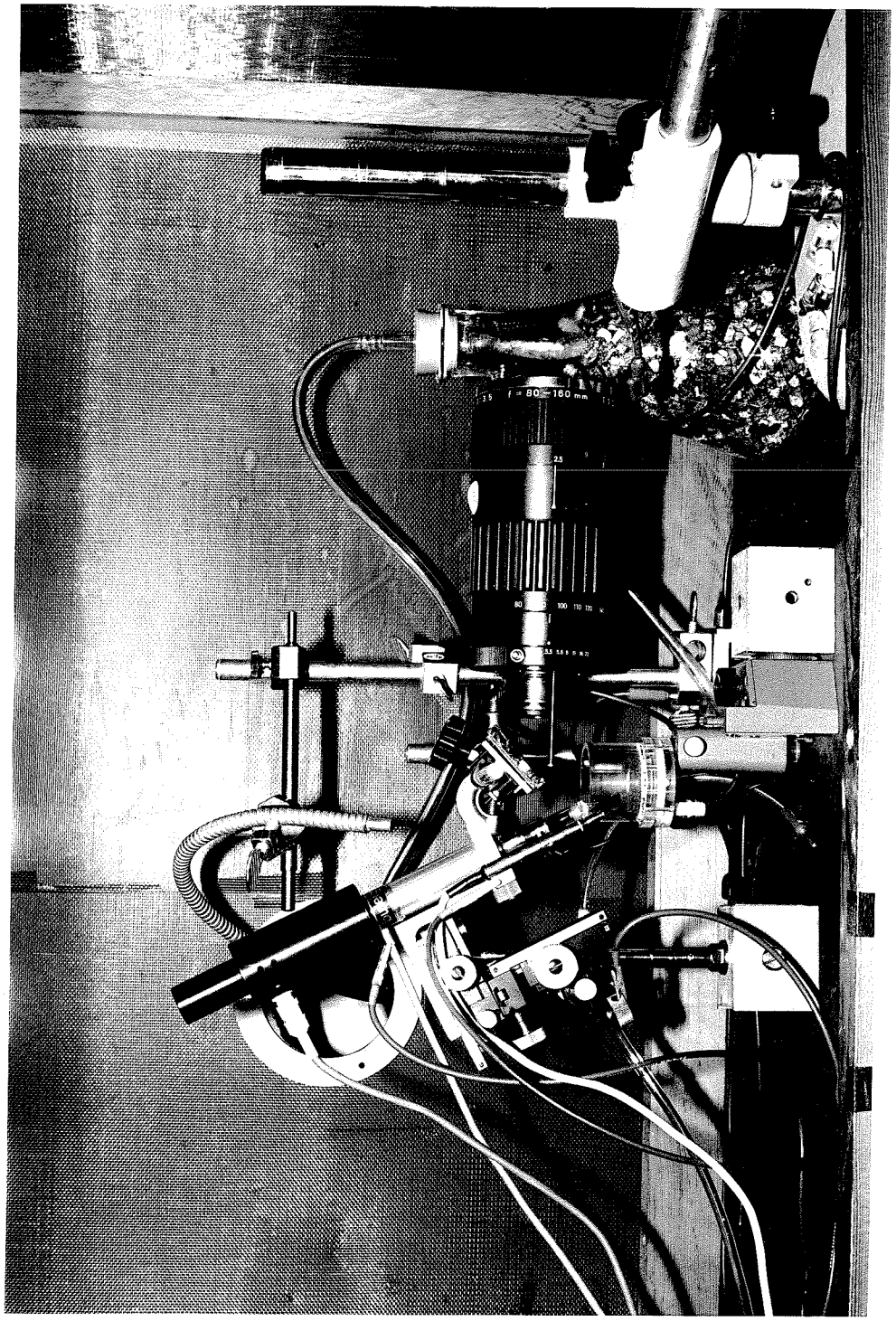

PLATE 3-1

diaminobenzidene and H_2O_2 and prepared for thick sectioning. After thick sectioning the tissue was mounted and the injected neuron was identified by light microscopy.

The stimulus was produced on a high intensity cathode ray tube (CRT) focused on the eyecup. The CRT had P4 phosphor of the sulfide type with a color temperature of 11,000 degrees Kelvin. The spectral-energy distribution characteristics for this phosphor are shown in figure 3-1.

The CRT controller was able to produce preset stimuli or display patterns prerecorded on digital tape. The preset stimuli were spots whose on and off times were controlled externally by a Grass model S4GR stimulator. Table 3-1 lists the sizes on the retina of the spots.

Table 3-1
SPOT SIZES ON RETINA

Spot Number	Diam.(microns)
1	83
2	416
3	667
4	830
5	1250

The patterns prerecorded on digital tape controlled a large 16 pixel by 16 pixel square. Each of the pixels was 93.75 microns wide at the surface of the retina. A new pattern could be presented each N x 10.6 milliseconds, where N is an integer. There were 16 intensity levels possible for each pixel.

The intensity of the stimulus was measured at each of the 16 levels using a Gamma Scientific telephotometer, Model 2000. A

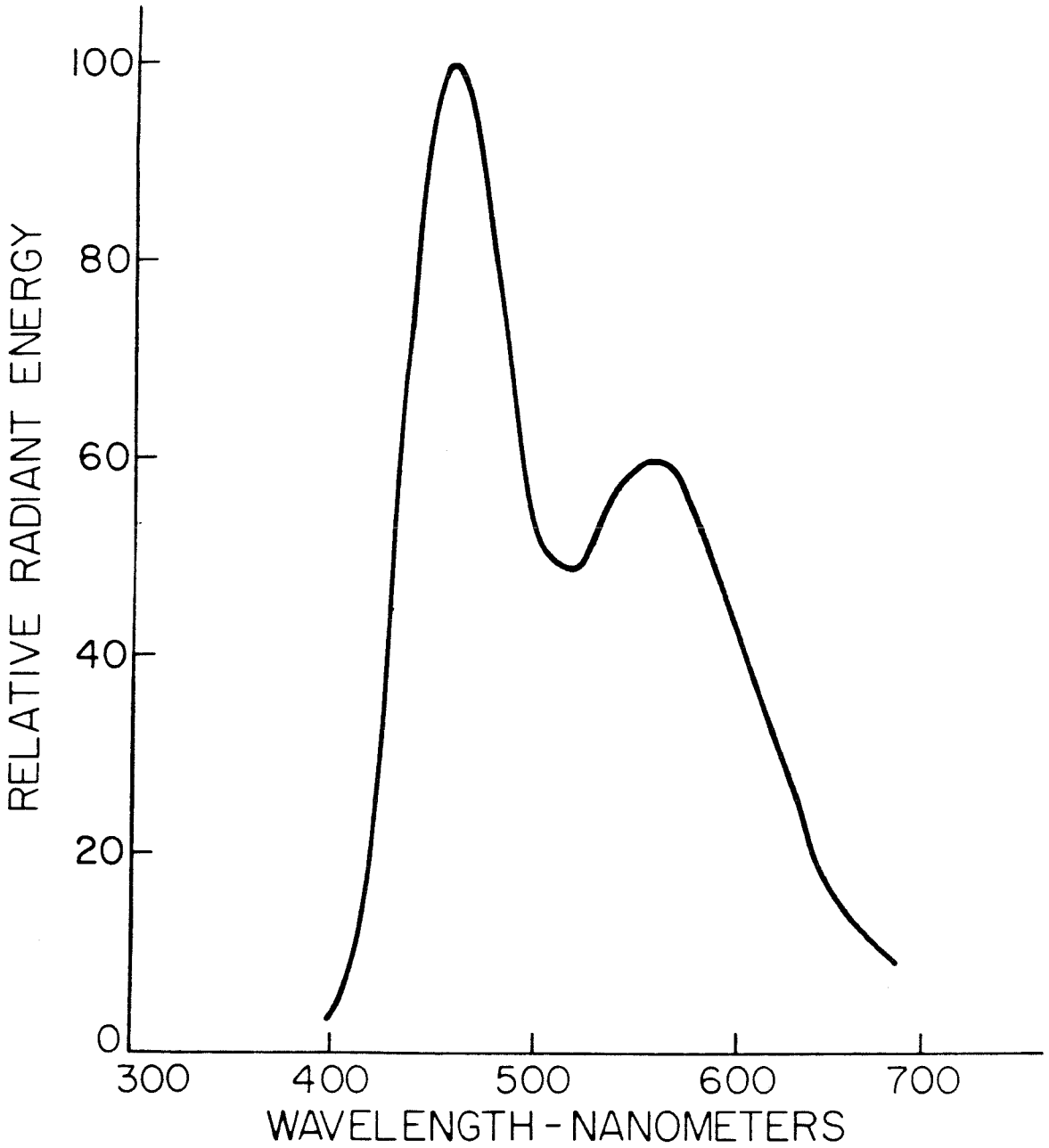

Figure 3-1 Spectral energy distribution characteristics for P4 phosphor of the sulfide type. Supplied by the manufacturer.

barium sulfate reflectance standard was placed in the position normally occupied by the eyecup so that the stimulus was in focus. The reflected light was measured using the telephotometer with a human photopic filter. Figure 3-2 is a plot of the measured intensity in photopic footlamberts versus the numerical designation of the level. Note that the levels are linearly related.

The signal from intracellular probing with the glass micropipette went into a low noise FET preamp and then into a negative capacitance amplifier, WPI model M701. This amplifier output the signal to various other amplifiers and devices at a gain of unity or five. The unit gain output went to a D.C. coupled chart recorder used to monitor drift of the cell's membrane potential. The output with amplification went to an amplifier whose gain could be set at 100 or 200. This amplifier applied a high pass filter with a cutoff frequency of 0.2 hertz and its output went to the data acquisition system. A complete block diagram of the recording equipment is shown in figure 3-3.

The data acquisition system consisted of a PDP-11/45 digital computer with a high speed 12 bit analog to digital converter. The amplified response was digitized online and stored on magnetic tape. Timing information for both the fixed stimuli and the prerecorded stimuli was recorded as well. The sampling interval for digitization was 0.01 seconds.

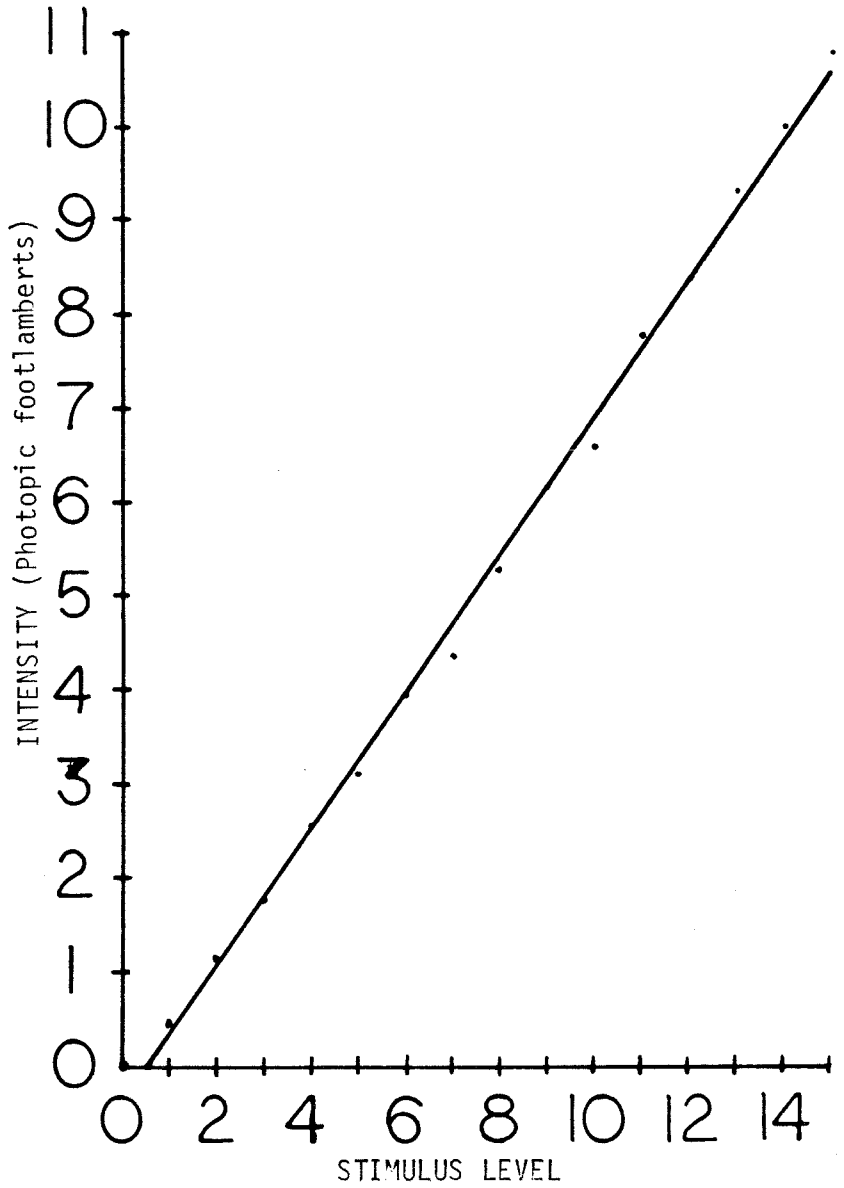

Figure 3-2 Relationship between stimulus level used in computations and the luminance of the stimulus measured at the position of the eyecup. The best fit line for the measured data is also shown. For the line the regression coefficient r=.998, the slope m=0.726, and the y intercept is -0.353.

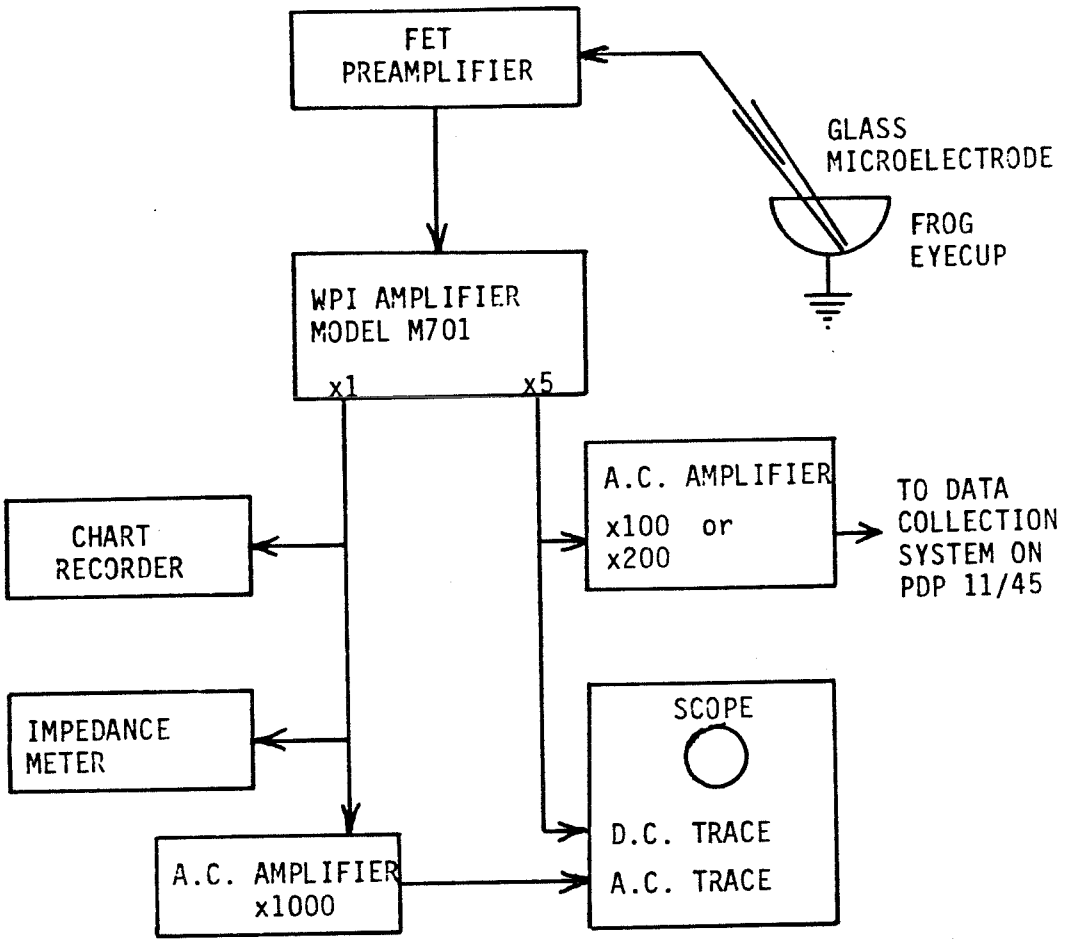

Figure 3-3 Block diagram of equipment used for intracellular recording in frog eyecup preparation.

3.2 ANALYTICAL

The recorded data were analyzed on a PDP-11/45 digital computer using the general analysis operating system (GAS). GAS has been developed over the past decade by programmers and researchers at Caltech. It provides a general set of programs for signal processing operations useful in performing the task of identifying specific systems. These operations include response averaging and calculation of Wiener kernels. There are also programs for modelling real and theoretical systems.

The experiments were performed using either conventional stimuli, such as flashing spots, or randomly modulated stimuli. The responses to conventional stimuli were averaged with stimulus onset as the trigger. The randomly modulated stimuli used were uniformly distributed 15 level random signals. It was found in practice that the responses to stimuli with a uniform distribution had a higher signal to noise ratio than the responses to stimuli with a gaussian distribution. The rest of this chapter presents a development of the algorithms for analyzing a system using a uniformly distributed N-level random input.

In recent years, the technique of non-parametric nonlinear system identification has been developed and successfully used on biological systems by several researchers [45,53,54,56,57]. In general the theoretical development of the technique has been in the continuous time domain using integral equations [53-57]. It is possible, however, to develop the entire theory for analyzing

nonlinear systems using random inputs in the discrete domain [44-46]. This formulation of the theory recognizes that the system will be analyzed with a digital computer using discrete experimental measurements of the systems output. Using the approach developed by Kroeker (1977) I will develop the set of orthogonal functionals describing a system stimulated by a uniformly distributed discrete random process with N levels. I will then show that these functionals may be evaluated using cross-correlation in the same manner as the Wiener functionals.

Let us consider the output, y(t), of an unknown system, F, which has x(t) as its input. We will assume that the system is causal and has finite memory. We wish to evaluate the way in which F maps past inputs $x(\tau)$, $t-M<\tau<t$, where M is the memory of the system, to y(t). The system will also be assumed to be time invariant, that is, the state of the system does not depend on initial conditions.

We will consider specifically the output of F resulting from an input which is an N-level uniformly distributed discrete random process. Such a process has the following properties:

a) If x is an element of the discrete random process the probability that x takes on one of the N possible discrete values is

$$P(x=x_i)) = 1/N \quad \text{where } x_i = 0,1,\ldots,N-1. \tag{1}$$

b) The mean μ of x is

$$\mu = (N-1)/2 \ . \tag{2}$$

c) The variance V is

$$V = (N-1)(N+1)/12 \ . \tag{3}$$

d) The joint density for independent samples is

$$P(x_1=x_i, x_2=x_j, \ldots, x_n=x_s) = N^{-s}. \tag{4}$$

We will make discrete measurements of the output y(t) and assume that we can sample fast enough so that these outputs will be an accurate representation of the response of F to x(t).

The orthogonal polynomials ϕ for a single uniformly distributed random variable are given by Jordan (1965):

$$\phi_m(x) = C_m \sum_{i=0}^{m+1} (-1)^{m-i} \binom{m+i}{m} \binom{N-i-1}{m-i} \binom{x}{i} \tag{5}$$

where $\binom{y}{j} = \dfrac{y(y-1)(y-2)\ldots(y-j+1)}{j!}$

and $\binom{y}{0} = 1$

The normalization constant C_m is determined by requiring the

variance of each polynomial to be unity. This leads to the following expression:

$$\frac{1}{N}\sum_{i=0}^{N}[\phi_m(x)]^2 = 1 = \frac{1}{N}C_m^2\binom{2m}{m}\binom{N+m}{m+1}$$

$$\text{or} \quad C_m = \left(\frac{1}{N}\binom{2m}{m}\binom{N+m}{m+1}\right)^{-.5} \qquad (6)$$

The first few polynomials are:

$$\phi_0 = 1$$

$$\phi_1 = V^{-.5}(x-\mu) \qquad (7)$$

$$\phi_2 = (.2(4V^2-V))^{-.5}[(x-\mu)^2-V)]$$

Suppose that out of a collection of S independent uniformly distributed variables $x_1,x_2,\ldots,x_s$ we pick n variables $x_{i_1},x_{i_2},\ldots,x_{i_n}$ where each i_k, k=1,2,...,n is chosen from 1,2,...,S and repetition is allowed. Let us define the multivariate uniform polynomial of $x_{i_1},x_{i_2},\ldots,x_{i_n}$ as [44,46,71]:

$$\Phi^n(x_{i_1},\ldots,x_{in}) = \prod_{\sigma=1}^{s}\phi_{n_\sigma}(x_\sigma); \qquad (8)$$

where n_σ is the number of times x_σ occurs in the collection $x_{i_1},x_{i_2},\ldots,x_{i_n}$ and the n_σ satisfy

$$\sum_{\sigma=1}^{s} n_\sigma = n$$

For example consider $\Phi^3(x_i,x_j,x_k)$:

$$\Phi^3(x_i,x_j,x_k) = \phi_1(x_i)\phi_1(x_j)\phi_1(x_k) \quad \text{if } i\neq j\neq k$$

$$= \phi_1(x_i)\phi_2(x_j) \quad \text{if } i\neq j=k$$

$$= \phi_3(x_i) \quad \text{if } i=j=k \qquad (9)$$

We define the expectation with respect to the joint density (4) as:

$$E[g(x_{i_1},\ldots x_{i_n})] = N^{-s}\sum_{x_1=0}^{N-1}\ldots\sum_{x_s=0} g(x_{i_1},\ldots x_{i_n})$$

THEOREM: The Φ have the following properties:

$$\Phi^0 = 1 \qquad (10)$$

$$E[\Phi^n] = 0 \qquad (11)$$

$$E[\Phi^n(x_{i_1},\ldots,x_{i_n})\Phi^m(x_{j_1},\ldots,x_{j_n})] = \delta_{nm}\delta^n_{ij} \qquad (12)$$

where $\delta_{nm} = 1$ for n=m and 0 otherwise, and $\delta^n_{ij} = 1$ if some permutation of $i_1,\ldots,i_n$ matches $j_1,\ldots,j_n$ and zero otherwise.

PROOF:

Equation (10) follows directly from equations (7) and (8). We show (11) by considering

$$E[\mathbb{a}^n] = E[\prod_{\sigma=1}^{s} \phi_{n_\sigma}(x_\sigma)] = E[\prod_{\sigma=0}^{s-1} \phi_{n_\sigma}(x_\sigma)]E[\phi_{n_s}(x_s)]$$

but $E[\phi_{n_s}(x_s)] = \frac{1}{N}\sum_{x_s=0}^{N-1} \phi_{n_s}(x_s) = 0$

by the way the ϕ_n are constructed. Therefore,

$$E[\mathbb{a}^n] = 0.$$

Using (8), (12) becomes

$$E[\mathbb{a}^n \mathbb{a}^{\dagger m}] = E[\prod_{\sigma=1}^{s} \phi_{n_\sigma}(x_\sigma)\phi_{m_\sigma}(x_\sigma)] \qquad (13)$$

where n_σ and m_σ are, respectively, the number of occurrences of σ in $i_1,\ldots,i_n$ and $j_1,\ldots,j_m$. We may rewrite this as

$$E[\mathbb{a}^n \mathbb{a}^{\dagger m}] = E[\prod_{\sigma=1}^{s-1} \phi_{n_\sigma}(x_\sigma)\phi_{m_\sigma}(x_\sigma)]E[\phi_{n_s}(x_s)\phi_{m_s}(x_s)]$$

but by the way the ϕ_n are constructed

$$E[\phi_{n_s}(x_s)\phi_{m_s}(x_s)] = \delta_{n_s m_s}$$

This argument could be repeated for $x_{s-1},\ldots,x_1$ yielding:

$$E[\mathbb{a}^n \mathbb{a}^{\dagger m}] = \prod_{\sigma=1}^{s} \delta_{n_s m_\sigma} = \delta_{nm}\delta^n_{ij}$$

proving (12). QED

We may now construct the functionals that will represent the system F. The relationship between the output of the system F and the functionals J_n is given by:

$$F(x_0, x_1, \ldots, x_M) = \sum_{n=0}^{N-1} J_n(f_n)$$

where

$$J_n(f_n) = \sum_{i_1=0}^{M} \cdots \sum_{i_n=0}^{M} f_n(i_1, \ldots, i_n) \Phi^n(x_1, \ldots, x_{i_n}) \qquad (14)$$

The f_n are the kernels of the system F. Note that the Φ^n are defined only for $n <= N-1$. Thus the functionals only provide a complete representation of the nonlinearities up to order N-1. This is a manifestation of the number of degrees of freedom in the N-level uniform stimulus.

We may now write out the first few functionals for the uniformly distributed input x(t) using equation (14). For the zero order case we have:

$$J_0 = f_0 \Phi^0 = f_0 \quad \text{since } \Phi^0 = 1 \qquad (15)$$

The first order case is a little more complicated. Using equation (14) again, now with n=1, we have:

$$J_1 = \sum_{i=1}^{M} f_1(i) \Phi^1(x_i).$$

But $\Phi^1 = \phi_1(x_i)$

So $$J_1 = V^{-.5} \sum_{i=1}^{M} f_1(i)(x_i - \mu) \qquad (16)$$

Now setting n=2 in equation (14) we may write out the second order functional J_2. Doing this we get:

$$J_2 = \sum_{i_1=1}^{M} \sum_{i_2=1}^{M} f_2(i_1,i_2)\Phi^2(x_{i_1},x_{i_2})$$

but $$\Phi^2(x_{i_1},x_{i_2}) = \prod_{\sigma=1}^{2} \phi_{n_\sigma}(x_\sigma)$$

$$= \phi_1(x_{i_1})\phi_1(x_{i_2}) \quad i_1 \neq i_2$$

$$= \phi_2(x_{i1}) \quad i_1 = i_2$$

We see from this that for $i_1 \neq i_2$, that is for off diagonal points, the multivariate polynomial is a product of first order single variable polynomials. For the on diagonal elements, $i_1 = 1_2$, the multivariate polynomial becomes the single variable second order polynomial ϕ_2. This illustrates the need for an adequate number of degrees of freedom in the stimulus. If the stimulus had a binary distribution then we would have N=2. From equation (5) we see that for N=2 ϕ_2 is equal to zero. Thus the diagonal elements of the second order nonlinearity would not be tested and as we shall see could not be evaluated.

Substituting from equation (7) we find that J_2 is

$$J_2 = V^{-1} \sum_{\substack{i_1=1 \\ i_1 \neq i_2}}^{M} \sum_{i_2=1}^{M} f_2(i_1,i_2)(x_{i_1}-\mu)(x_{i_2}-\mu)$$

$$+ (.2(4V^2-V))^{-.5} \sum_{\substack{i_1=1 \\ i_1=i_2}}^{M} f_2(i_1,i_1)((x_{i_1}-\mu)^2-V) \qquad (17)$$

3.2.1 Calculation of the kernels

Consider the expected value of y(t). By the way that the series has been constructed the expected value operation on y(t) will yield f_0 the zero order kernel for the system. We may write then:

$$f_0 = E[y(t)] \tag{18}$$

Now consider $E[F(x_0,\ldots,x_M)(x_\sigma-\mu)]$. Substituting from equation (14) we have:

$$E[F(x_0,\ldots,x_M)(x_\sigma-\mu)] = \tag{19}$$

$$E[\sum_{n=0}^{N-1} J_n(x_{i_1},\ldots,x_{i_n})(x_\sigma-\mu)] =$$

$$E[\sum_{n=0}^{N-1}\sum_{i_1=0}^{M}\ldots\sum_{i_n=0}^{M} f_n(i_1,\ldots,i_n)\mathcal{H}^n(x_{i_1},\ldots,x_{i_n})(x_\sigma-\mu)]$$

but by construction the $\mathcal{H}^n$ are orthogonal to all polynomials of lower order, so this becomes

$$E[f_0(x_\sigma-\mu)] + E[\sum_{i_1=0}^{M} f_1(i_1)\mathcal{H}^1(x_{i_1})(x_\sigma-\mu)] =$$

$$0 + E[k_1 \sum_{i_1=0}^{M} f_1(i_1)(x_{i_1}-\mu)(x_\sigma-\mu)]$$

Where $k_1 = V^{-.5}$

Taking the expected values inside we have:

$$k_1 \sum_{i_1=0}^{M} f_1(i_1) E[(x_{i_1}-\mu)(x_\sigma-\mu)] =$$

$$k_1 \sum_{i_1=0}^{M} f_1(i_1) V\delta_{i_1\sigma}$$

So (19) becomes:

$$1/k_1 f_1(\sigma)$$

rearranging we have:

$$f_1(\sigma) = V^{-.5} E[F\ (x_\sigma-\mu)] \qquad (20)$$

Now let us figure out how to calculate the second order kernel by considering $E[F\ (x_{\sigma_1}-\mu)(x_{\sigma_2}-\mu)]$. Substituting from equation (14) we have:

$$E[F\ (x_{\sigma_1}-\mu)(x_{\sigma_2}-\mu)] = \qquad (21)$$

$$E[\sum_{n=0}^{N-1} J_n(x_{i_1},\ldots,x_{i_n})(x_{\sigma_1}-\mu)(x_{\sigma_2}-\mu)\ ] =$$

$$E[\ f_0\ (x_{\sigma_1}-\mu)(x_{\sigma_2}-\mu)] +$$

$$E[\ k_1 \sum_{i_1=0}^{M} f_1(i_1)(x_{i_1}-\mu)(x_{\sigma_1}-\mu)(x_{\sigma_2}-\mu)\ ] +$$

$$E[\ k_1^2 \sum_{\substack{i_1=0 \\ i_1\neq i_2}}^{M}\sum_{i_2=0}^{M} f_2(i_1,i_2)(x_{i_1}-\mu)(x_{i_2}-\mu)(x_{\sigma_1}-\mu)(x_{\sigma_2}-\mu)]+$$

$$E[\ k_2 \sum_{i_1=0}^{M} f_2(i_1,i_1)((x_{i_1}-\mu)^2-k_1^{-2})(x_{\sigma_1}-\mu)(x_{\sigma_2}-\mu)\ ]$$

Considering the first term of this expression we find:

$$E[\ (x_{\sigma_1}-\mu)(x_{\sigma_2}-\mu)\ ] =$$

$$f_0 E[\ (x_{\sigma_1}-\mu)(x_{\sigma_2}-\mu)\ ] = f_0\ \delta_{\sigma_1\sigma_2} V$$

We see that when $\sigma_1=\sigma_2$ this term will be non zero. Now considering the second term we find:

$$E[\ k_1 \sum_{i_1=0}^{M} f_1(i_1)(x_{i_1}-\mu)(x_{\sigma_1}-\mu)(x_{\sigma_2}-\mu)\ ] =$$

$$k_1 \sum_{i_1=0}^{M} f_1(i_1)\ E[\ (x_{i_1}-\mu)(x_{\sigma_1}-\mu)(x_{\sigma_2}-\mu)\ ]$$

$$= 0$$

The second term will have no effect on the calculations because it goes to zero. Considering the third term and performing the expected value operation we find:

$$E[\ k_1^2 \sum_{i_1=0}^{M}\sum_{i_2=0}^{M} f_2(i_1,i_2)(x_{i_1}-\mu)(x_{i_2}-\mu)(x_{\sigma_1}-\mu)(x_{\sigma_2}-\mu)\ ]$$

$$= k_1^2 \sum_{\substack{i_1=0 \\ i_1\neq i_2}}^{M}\sum_{i_2=0}^{M} f_2(i_1,i_2) E[\ (x_{i_1}-\mu)(x_{i_2}-\mu)(x_{\sigma_1}-\mu)(x_{\sigma_2}-\mu)\ ]$$

$$= k_1^2 \sum_{\substack{i_1=0 \\ i_1\neq i_2}}^{M}\sum_{i_2=0}^{M} f_2(i_1,i_2) V^2\ (\delta_{i_1 i_2}\delta_{\sigma_1\sigma_2} + \delta_{i_1\sigma_1}\delta_{i_2\sigma_2} + \delta_{i_1\sigma_2}\delta_{i_2\sigma_1})$$

$$= k_1^{-2}\ [f_2(\sigma_1,\sigma_2) + f_2(\sigma_2,\sigma_1)] \qquad \sigma_1\neq\sigma_2$$

but f_2 is symmetric so the third term becomes:

$$2k_1^{-2}\ f_2(\sigma_1,\sigma_2) \qquad \sigma_1\neq\sigma_2$$

We now have the formulation for calculating the off diagonal elements of the second order kernel f_2. Finally if we consider the fourth term and perform the expected value operation we find:

$$E[\, k_2 \sum_{i_1=0}^{M} f_2(i_1,i_1)((x_{i_1}-\mu)^2-k_1^{-2})(x_{\sigma_1}-\mu)(x_{\sigma_2}-\mu)\,]$$

$$= k_2 \sum_{i_1=0}^{M} f_2(i_1,i_1)E[\,(x_{i_1}-\mu)(x_{i_1}-\mu)(x_{\sigma_1}-\mu)(x_{\sigma_2}-\mu)\,] - k_2k_1^{-2} \sum_{i_1=0}^{M} f_2(i_1,i_1)E[\,(x_{\sigma_1}-\mu)(x_{\sigma_2}-\mu)\,]$$

$$= k_2 \sum_{i_1=0}^{M} f_2(i_1,i_1)\, V^2\, (\delta_{\sigma_1\sigma_2} + \delta_{i_1\sigma_1}\delta_{i_1\sigma_2} + \delta_{i_1\sigma_2}\delta_{i_1\sigma_1}) - k_2k_1^{-2} \sum_{i_1=0}^{M} f_2(i_1,i_1)\, V\, \delta_{\sigma_1\sigma_2}$$

but $k_1 = V^{-.5}$, so we have:

$$2k_1^{-4}k_2 f_2(\sigma_1,\sigma_1) \qquad \sigma_1=\sigma_2$$

Recall that we found that the first term makes a contribution to the calculation when $\sigma_1=\sigma_2$. The calculation of the diagonal of the second order kernel will, therefore, be off by f_0V unless we subtract f_0 from the response before the calculation of f_2. If we do that then we have the following formulas for calculating the second order kernel:

$$f_2(\sigma_1,\sigma_2) = \frac{1}{2V} E[\,(F-f_0)(x_{\sigma_1}-\mu)(x_{\sigma_2}-\mu)\,] \quad \sigma_1\neq\sigma_2 \quad (22)$$

$$f_2(\sigma_1,\sigma_1) = \frac{k_2}{2V^2} E[\,(F-f_0)(x_{\sigma_1}-\mu)(x_{\sigma_2}-\mu)\,] \quad \sigma_1=\sigma_2 \quad (23)$$

Since we are dealing with a stationary system and since x is ergodic we may use index averaging in place of the expected value operation. In practice the data set is usually a sampled signal and the index then is the multiplier of the sample increment. Under these conditions the algorithms for computation of the kernels are:

$$J_0: \quad f_0 = \frac{1}{N}\sum_{n=0}^{N-1} y(t_n) \tag{24}$$

$$J_1: \quad f_1(\sigma) = \frac{V}{N}^{-.5}\sum_{n=0}^{N-1} (y(t_n)-f_0)(x(t_n-\sigma)-\mu) \tag{25}$$

$$J_2: \quad f_2(\sigma_1,\sigma_2) = \frac{1}{2NV}\sum_{n=0}^{N-1} (y(t_n)-f_0)(x(t_n-\sigma_1)-\mu)(x(t_n-\sigma_2)-\mu) \quad \sigma_1\neq\sigma_2 \tag{26}$$

and

$$f_2(\sigma_1,\sigma_1) = \frac{(.2(4V^2-V))^{-.5}}{2NV^2}\sum_{n=0}^{N-1}(y(t_n)-f_0)(x(t_n-\sigma_1)-\mu)(x(t_n-\sigma_2)-\mu) \quad \sigma_1=\sigma_2 \tag{27}$$

where N is the number of points in the response data set.

The uniform functionals may be extended to multi-input systems just as the Wiener functionals were by Marmarelis and McCann (1973) and Marmarelis and Naka (1974). This leads to terms in the second order and higher functionals which result from nonlinear interaction between the different inputs. This interaction term is called a mutual- or cross-kernel. There are also additional individual terms in each functional for each input. These are called self-kernels.

In J_2 the cross-kernel appears as:

$$V^{-1} \sum_{i_1=0}^{M} \sum_{i_2=0}^{M} f_{xu}(i_1,i_2)(x_{i_1}-\mu_x)(u_{i_2}-\mu_u)$$

where x and u are the two inputs which are randomly modulated and independent of each other. The cross kernel is calculated using the following formula:

$$f_{xu}(\sigma_1,\sigma_2) = \frac{1}{NV} \sum_{n=0}^{N-1} (y(t_n)(x(t_n-\sigma_1)-\mu_x)(x(t_n-\sigma_2)-\mu_u) \quad (28)$$

4. RESULTS

This chapter describes the results from intracellular recordings of frog photoreceptors and L-type horizontal cells. Plates 4-1 and 4-2 show the results of injections with HRP in two cone photoreceptors. The cell in plate 4-1 was injected by iontophoresis for 10 seconds at a current of 5 nanoamps. It was processed as described in section 3.1 and cut in 40 micron thick sections. The cone is approximately 10 microns in diameter and 60 microns long. The cell in plate 4-2 was also injected by iontophoresis. It was injected for 5 seconds at 5 nanoamps at the end of two hours of recording. This was the longest recording made from any one cell. It recovered its response completely after the injection. It was injected a second time for 5 seconds at 5 nanoamps twenty minutes after the first injection. An internal horizontal cell was also stained but not recorded from in this retina. It appears to have been penetrated during the advancement of the electrode and to have taken up extracellular HRP. Both cones have the characteristic oil droplet and conical outer segment.

The following sections describe the electrophysiological results. Each section describes the stimulus used and then the response of the photoreceptors and horizontal cells to that stimulus.

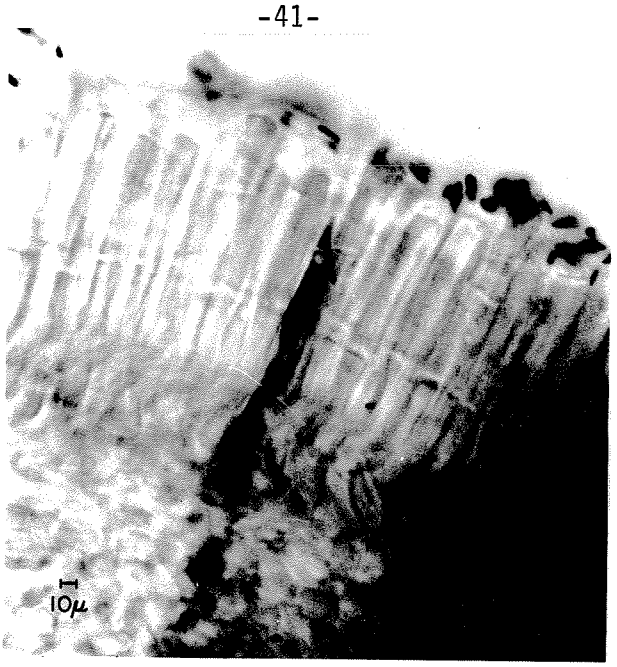

PLATE 4-1

PLATE 4-2

4.1 ADAPTATION OF CENTER BY SURROUND

This experiment was a first attempt to test the hypothesis that illumination in the surround of a photoreceptor's receptive field affects the state of adaptation of the photoreceptor. The stimulus was configured with the central 4 pixels as the 'center' and all the other pixels of the 16x16 pattern as 'surround'. The cell's sensitivity was measured by flashing the center from its steady state level to each of the other levels, 0 to 15. This presentation was made 3 times for each set of conditions. The responses were analyzed by averaging and then plotting the peak response to each stimulus level versus the logarithm of the intensity at that level in footlamberts.

The experiment was carried out for three sets of conditions. The first set of conditions provided a baseline measurement of the cell's sensitivity at low levels of steady illumination. For this step the center and surround steady state level was 0 (BG0CT0). The second measurement was made with the center adapted to a slightly higher level of illumination, level 3. The surround was kept steady at level 0 (BG0CT3). The last measurement was made with center and surround both having a steady state intensity of level 3 (BG3CT3).

This experiment was performed on four cone photoreceptors. Figure 4-1 shows a set of typical results for this experiment. The data points for level 0 are not plotted to minimize compression of the results by the logarithmic scale. The figure shows

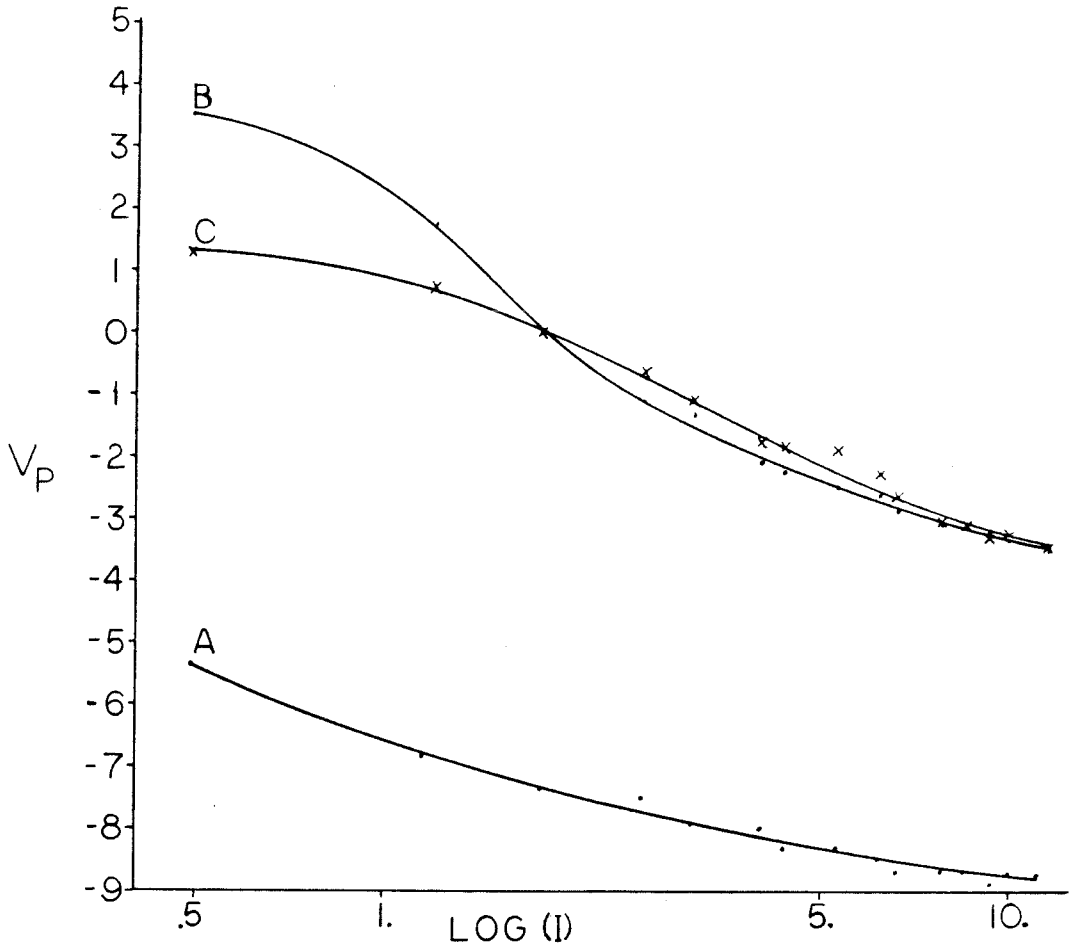

Figure 4-1 Intensity - response curves for a cone photoreceptor. A: Background level 0, center level 0. B: Background level 0, center level 3. C: Background level 3, center level 3. The center was the 2 pixel by 2 pixel center of 16 by 16 pattern. The background was the rest of the 16 by 16 pattern. One pixel was 93.75 microns wide at the eyecup position. Sensitivity was tested by flashing the center from resting level to each of the other 15 levels. V_p is the peak response, in millivolts, at each level. The horizontal scale is in logfootlamberts.

that there is a slight compression of response for BG3CT3 as compared to BG0CT3. Notice also the large change in the curve from BG0CT0 to the other two conditions. The intensity at level 0 is -3.68 log-footlamberts.

4.2 Random Rings - No Desensitization

The stimulus used for this set of experiments is illustrated in figure 4-2. It was of a pattern of eight concentric square rings. The center ring, R0, was a 2 pixel by 2 pixel spot. Around it were seven square rings, R1 - R7, each 1 pixel wide. Each of the eight rings was independently modulated by a uniformly distributed random process.

Figure 4-3 shows the eight first order kernels for a cone photoreceptor. These kernels are initially hyperpolarizing, that is they go from a resting level to a negative level and then back to the resting level. The kernels are typical of the kernels obtained by recording from five other photoreceptors.

A cell's receptive field is usually determined by measuring the peak response to a small spot at various positions. Figure 4-4 illustrates a new way to describe a cell's receptive field. The values along the vertical axis are determined by taking the ratio of response per unit area in ring Rn to the response per unit area in R0. The response per unit area is determined by dividing the peak polarization of the first order kernel for each ring by the number of pixels, or area, of that ring. This figure shows that the receptive field of the photoreceptors fell

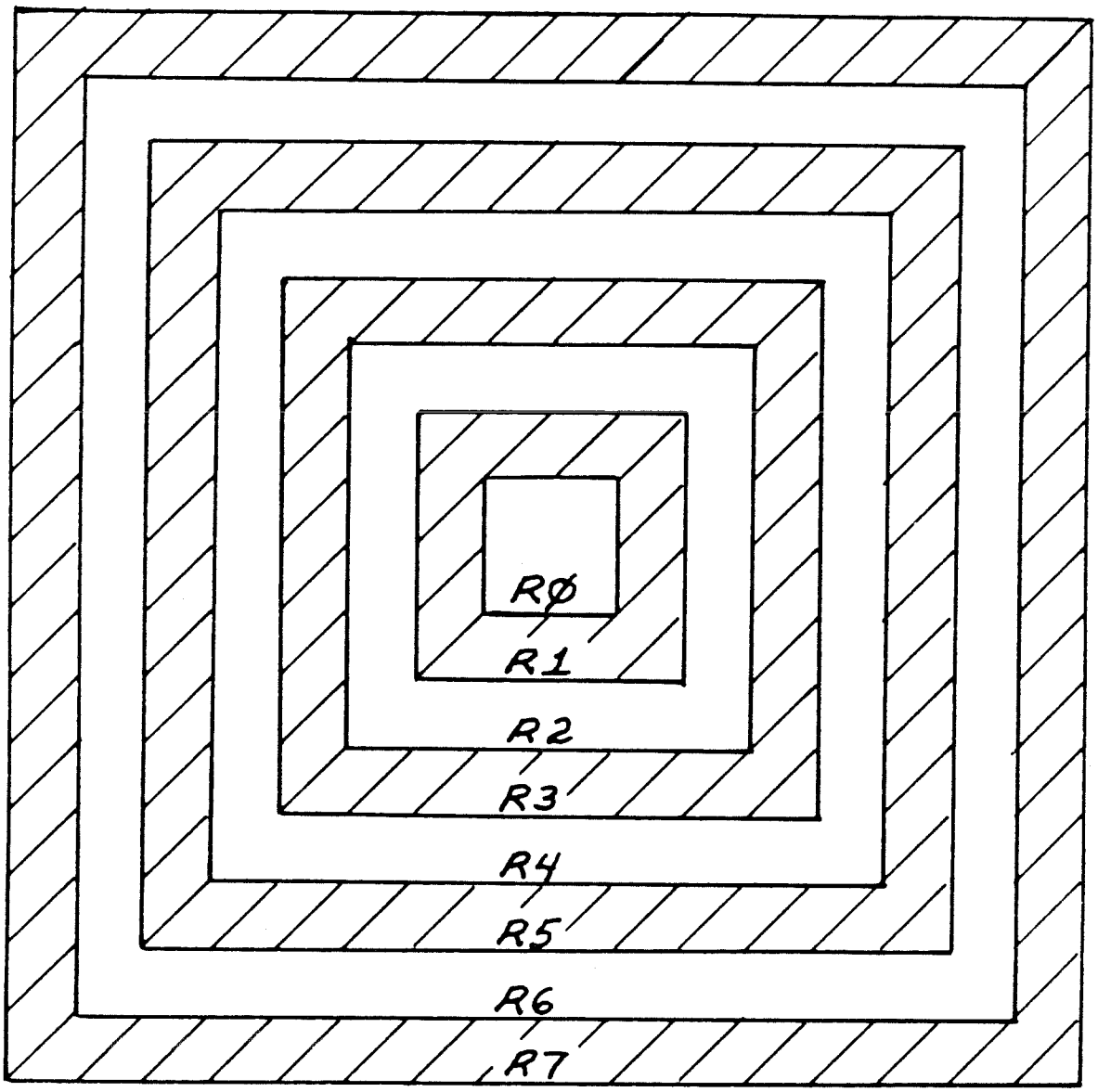

Figure 4-2 Representation of the stimulus configuration for experiments presented in sections 4.2 and 4.4 of the text. RO is 2 pixels square and each of the other rings is 1 pixel wide. At the eyecup position 1 pixel was measured as 93.75 microns wide.

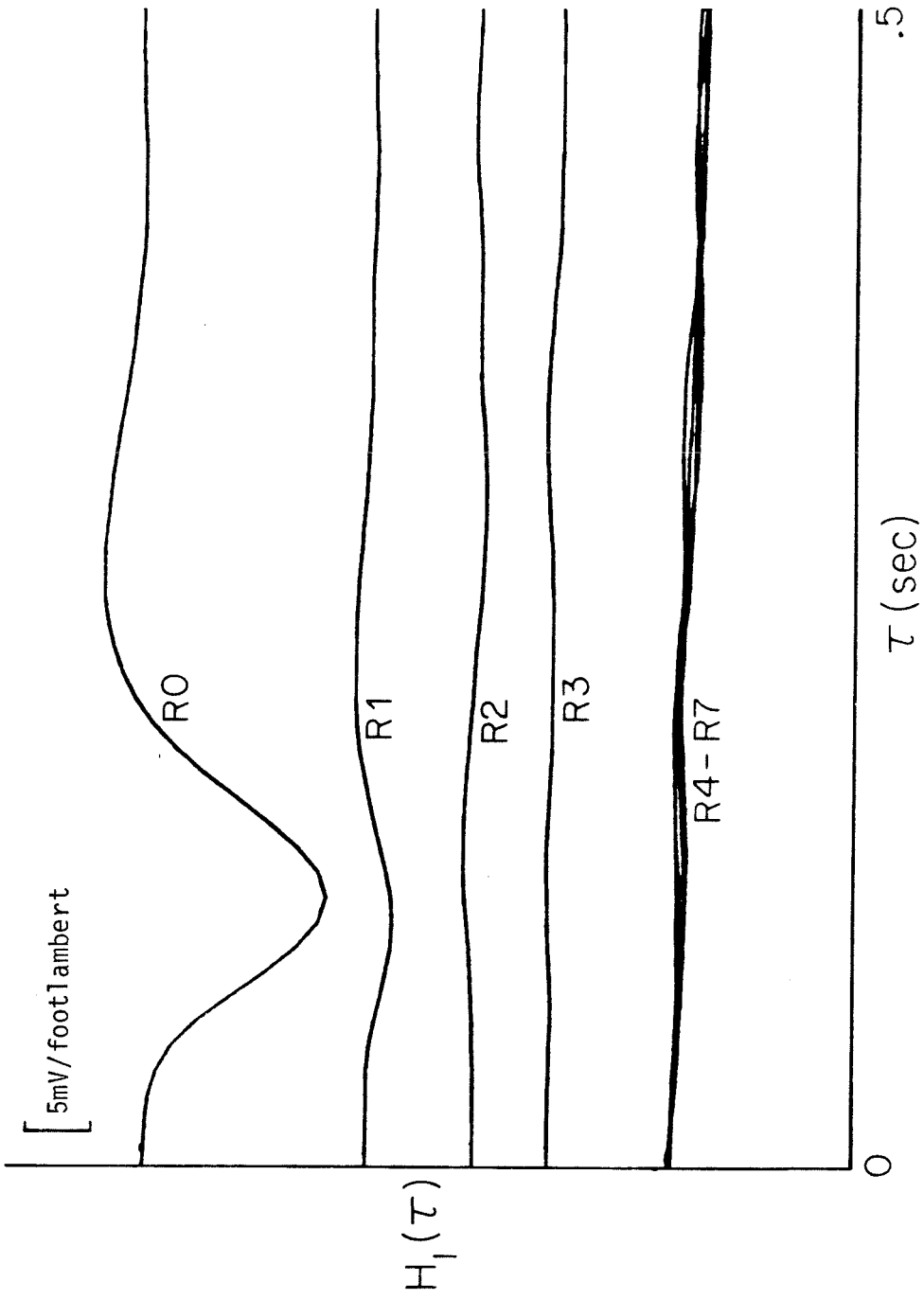

Figure 4-3 First order kernels for a cone photoreceptor. Stimulus was configured as shown in fig.4-2. Each ring, R0-R7, was independently modulated by a 15 level uniformly distributed random signal.

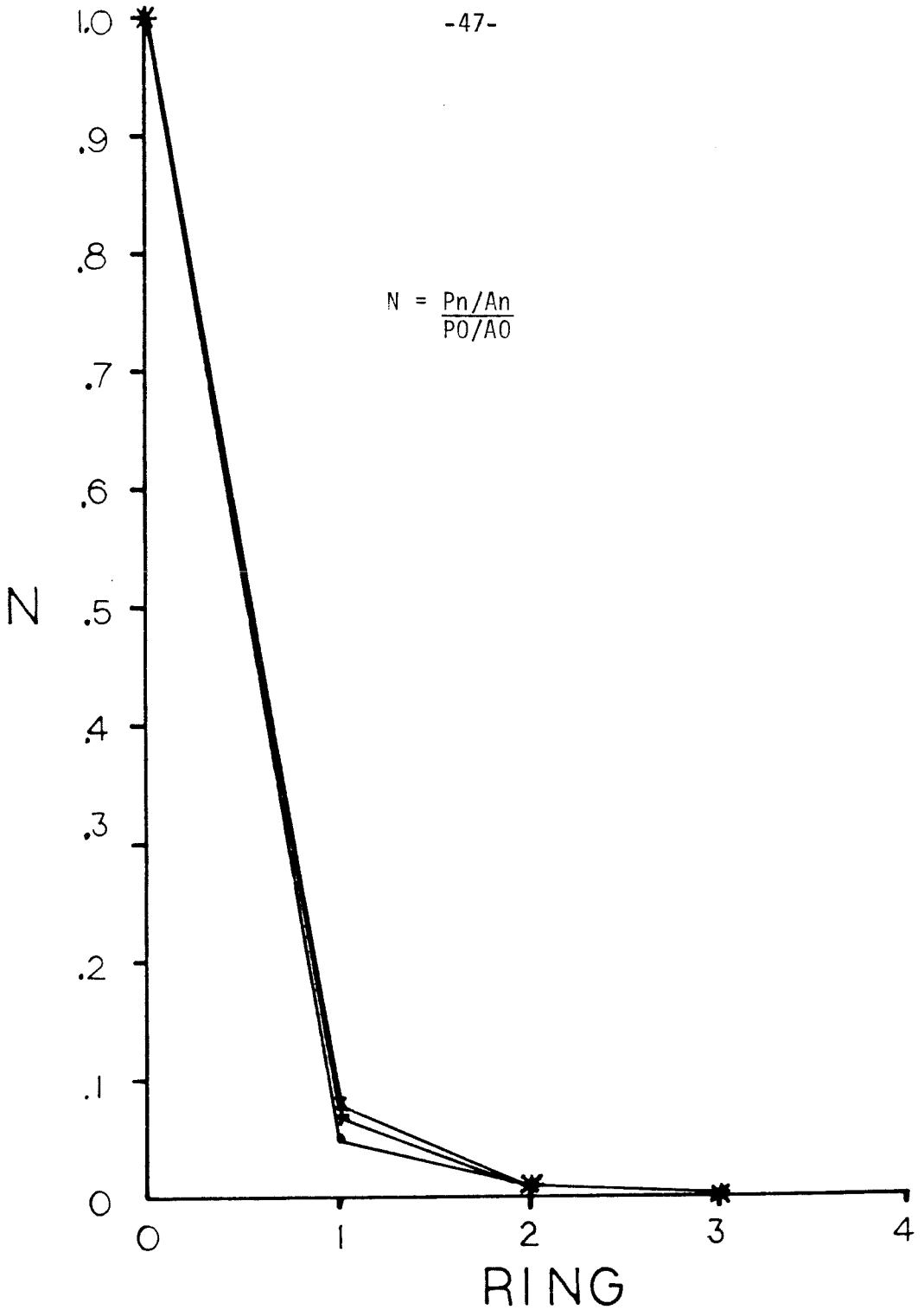

Figure 4-4 Receptive field plot for three cone photoreceptors. Pn is the peak of the first order kernel for ring Rn, P0 for R0. An is the area of ring Rn, A0 of R0. This plot was constructed using the first order kernels shown in fig. 4-3 for one of the cones and kernels not shown for the other two cones.

entirely within R0.

Figure 4-5 A shows the second order self-kernel of R0 for the same cell as the previous figures. The second order kernel is depolarizing, that is it goes from rest to a positive peak and then back to rest. This indicates that the nonlinearity decreases the overall response of the system since the first and second order kernels are of opposite polarity. It peaks at approximately the same time as the first order kernels.

Figure 4-5 B shows the cross-kernel between R0 and R1. The cross kernel is also depolarizing indicating that illumination of one ring R1 suppresses the response due to illumination of R0.

Table 4-1 presents the results of modeling this cell's response to the uniformly distributed random stimulus and comparing it with the cell's actual response. To find the dynamic mean square error, MSE, both signals are adjusted to have zero mean. Then the variance of the difference between the adjusted signals is computed. This variance is the dynamic MSE. The percent dynamic MSE is the ratio of the dynamic MSE to the variance of the adjusted actual response. This is inversely related to the signal to noise ratio. The results of this comparison indicate that only the kernels for rings R0 and R1 are significant. Figure 4-6 compares sections from the modeled response and the actual response.

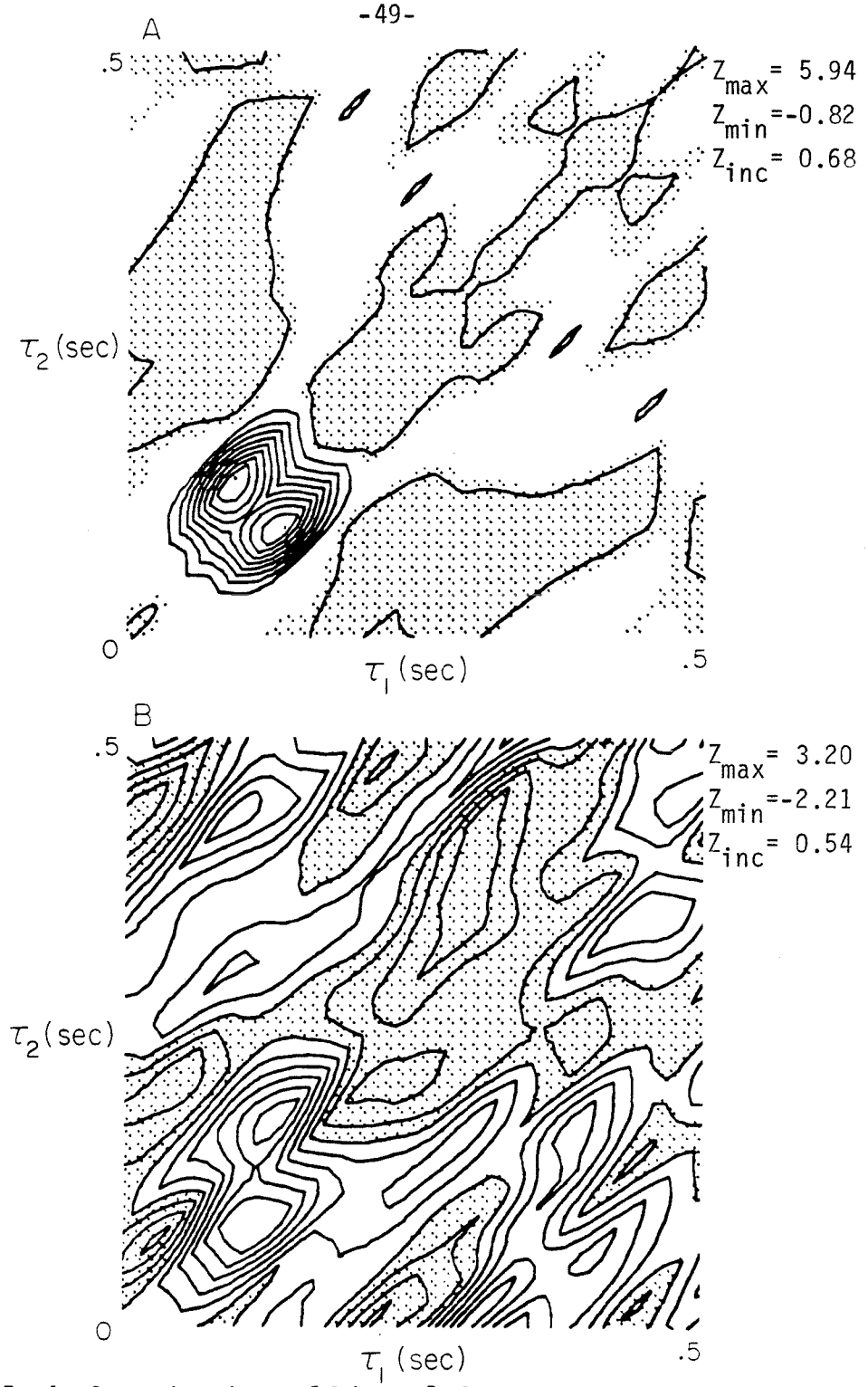

Figure 4-5 A: Second order self kernel for a cone photoreceptor.

B: Second order cross kernel between R0 and R1, also for a cone photoreceptor. R0 corresponds to τ_1, R1 to τ_2. The Z axis contour units are mV/(footlambert)^2. Stippling denotes negative areas.

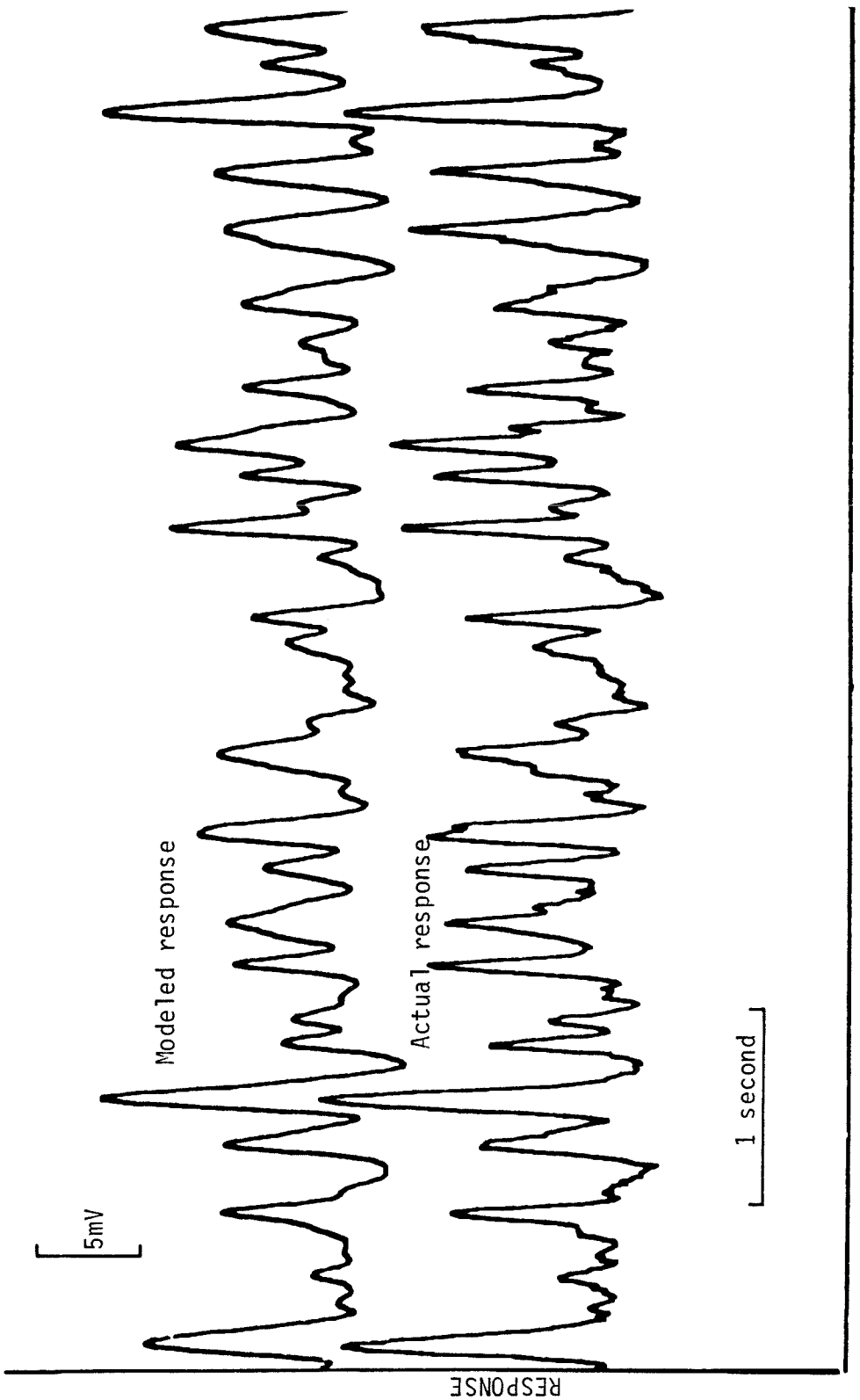

Figure 4-6 Modeled response and actual response of cone photoreceptor to the uniformly distributed random stimulus. The modeled response was computed using the kernels shown in figures 4-3 and 4-5.

Table 4-1
Cone Photoreceptor Model Comparison

Kernels Used for Model				Dynamic MSE	Pct. Dynamic MSE
R0	H1			0.4419	19.55
R0->R1	H1			0.4123	18.24
R0->R2	H1			0.4101	18.15
R0->R3	H1			0.4122	18.24
R0->R4	H1			0.4121	18.24
R0->R5	H1			0.4117	18.22
R0->R6	H1			0.4104	18.16
R0->R7	H1			0.4128	18.27
R0->R6	H1	R0	H2	0.2984	13.20
R0->R6	H1	R0->R1	H2	0.3015	13.34
R0->R6	H1	R0->R1	H2+H2R0XR1	0.3174	14.04

Figure 4-7 shows the eight first order kernels for a horizontal cell. As was shown for the photoreceptors, these kernels are hyperpolarizing. Note that for the horizontal cell there are non-zero kernels beyond R1. This is typical of horizontal cell kernels because the horizontal cells have much larger receptive fields than the photoreceptors. For this particular cell the kernels are apparent for all eight rings.

Figure 4-8 is a plot of the receptive field for two horizontal cells tested with this stimulus. This figure was constructed in the same manner as figure 4-4. One of the cells shows the largest response in ring R1. This is probably a result of the product of the spatial weighting function and area having a maximum off center.

Table 4-2 shows the results of modeling of one of these cell's response to the uniformly distributed random stimulus. One thing apparent from the modeling is that the second order self kernels are weak for this horizontal cell. Figure 4-9 compares sections from the actual and modeled response to the random

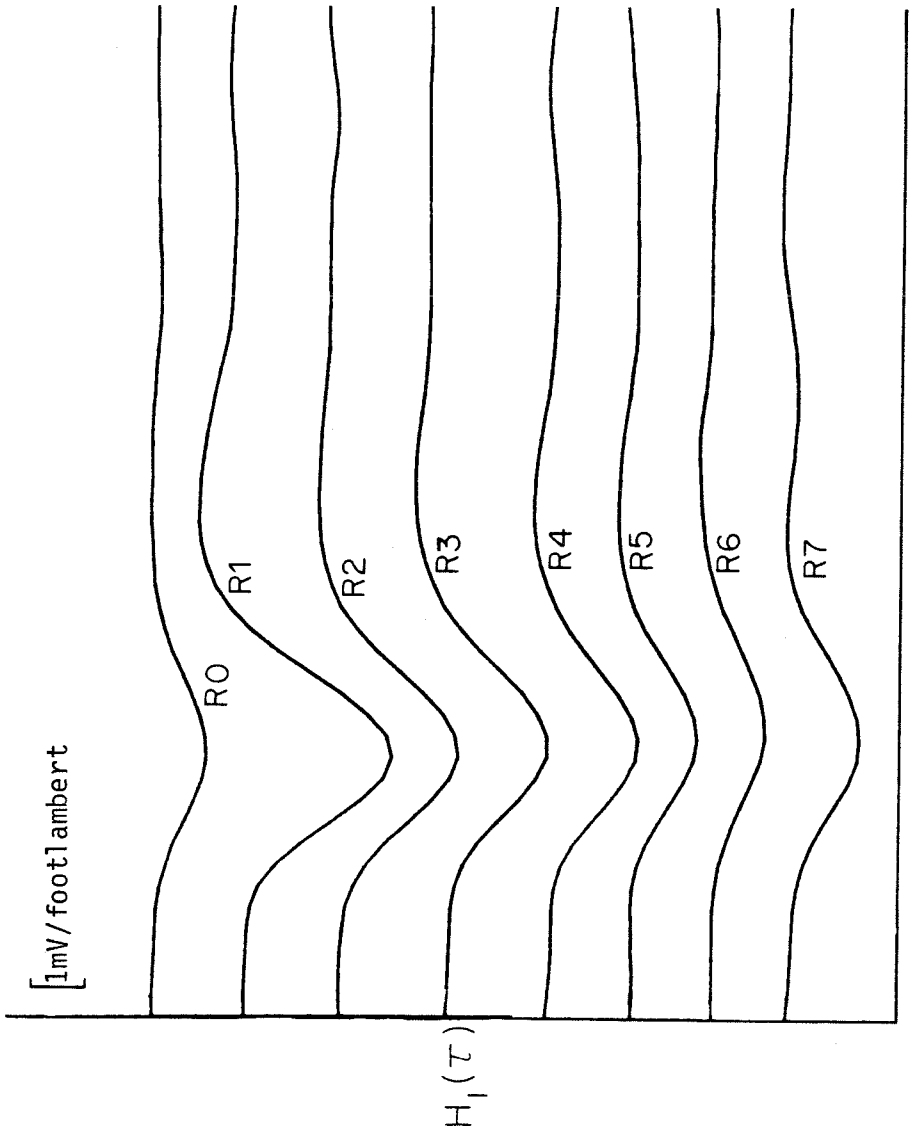

Figure 4-7 First order kernels for a horizontal cell. Stimulus was configured as shown in fig. 4-2. Each ring, R0-R7 was independently modulated by a 15 level uniformly distributed random signal.

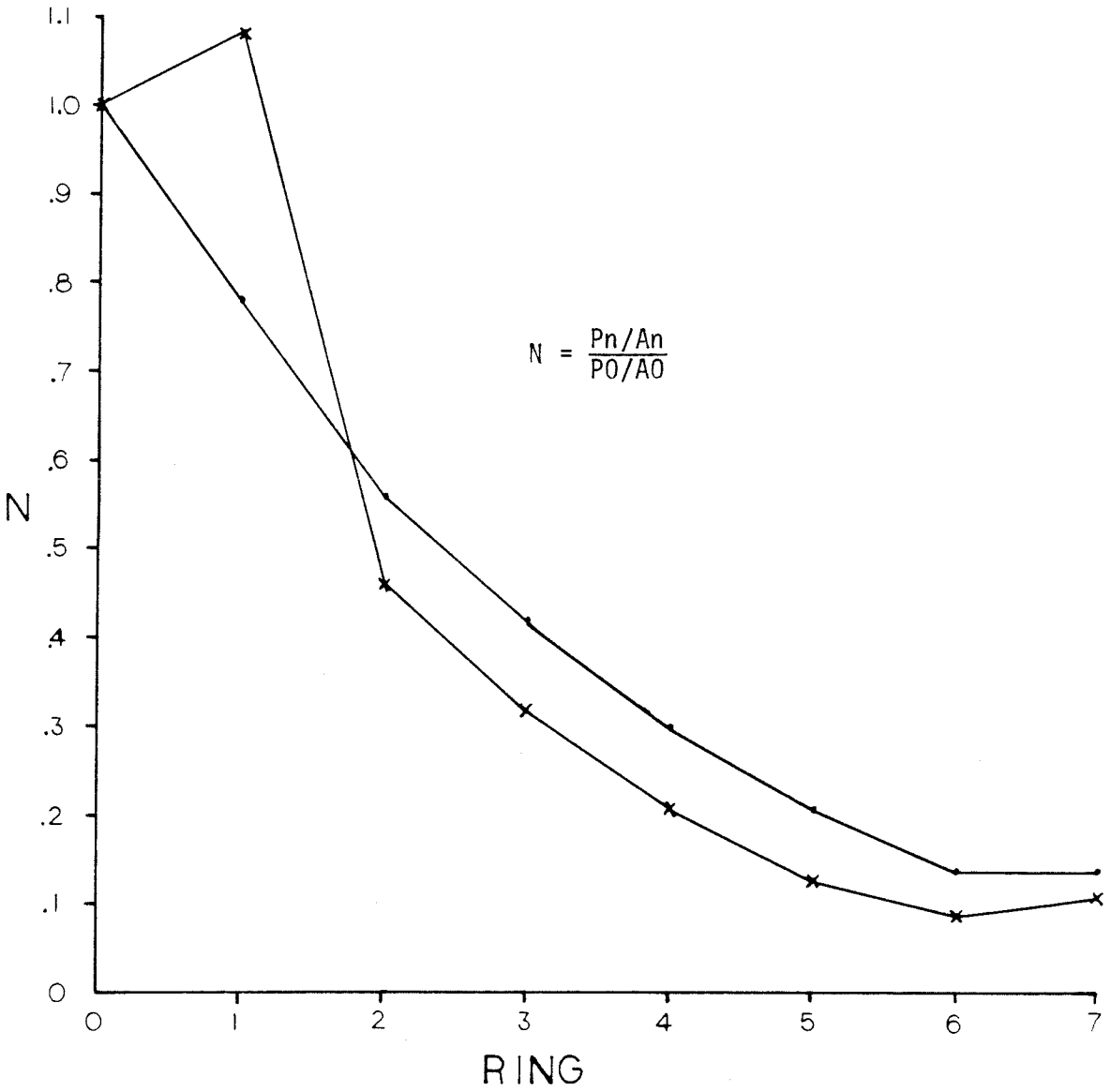

Figure 4-8 Receptive field plot for two horizontal cells. Pn is the peak of the first order kernel for ring Rn and P0 for R0. An is the area of ring Rn and A0 of R0. The distance between ring centers was 93.75 microns at the eyecup position.

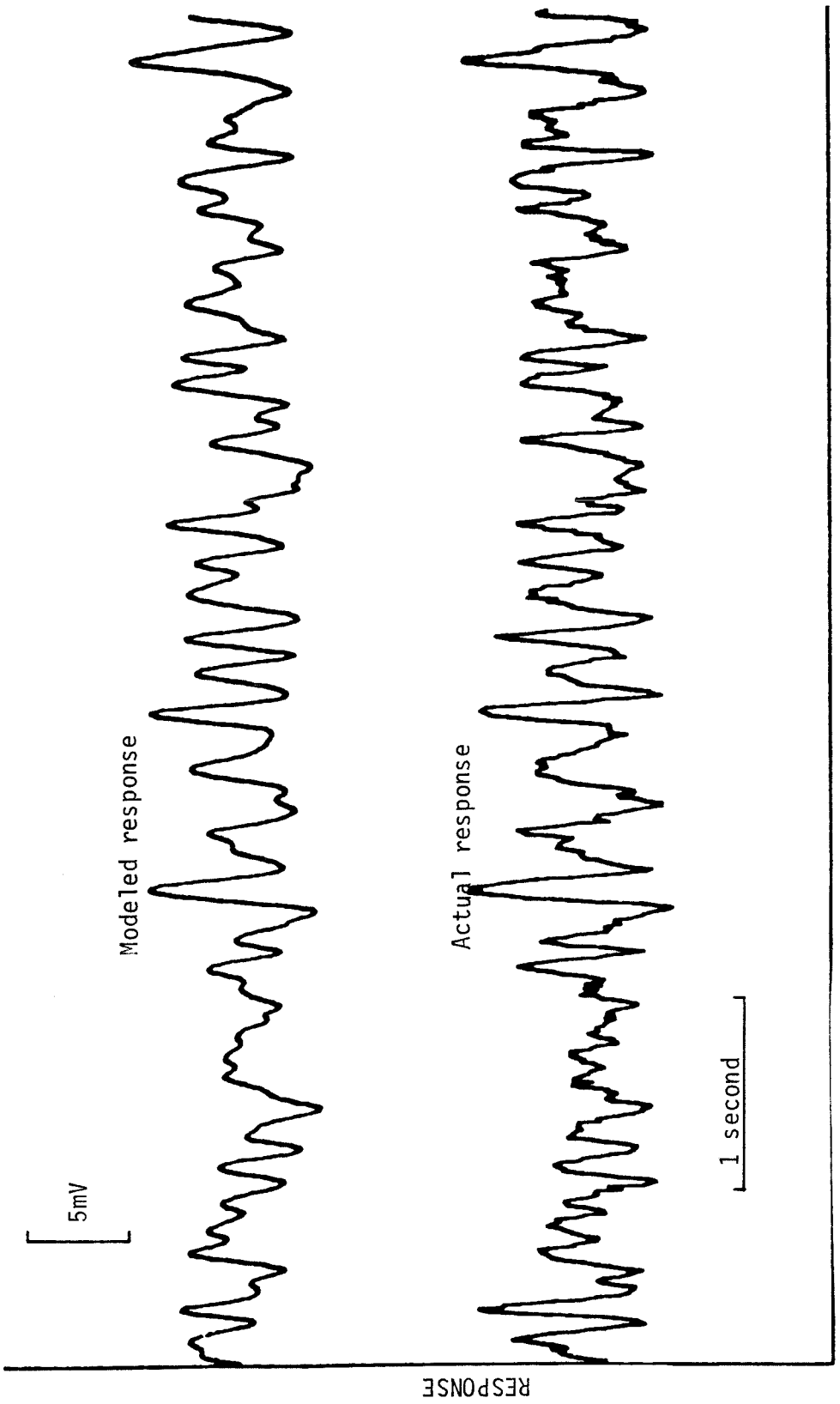

Figure 4-9 Modeled response and actual response of a horizontal cell to the uniformly distributed random stimulus. The modeled response was computed using the kernels shown in figure 4-7.

stimulus. The figure shows that the modeled response is in good agreement with the actual response. The main apparent difference is that the actual response has a component of high frequency noise which is not present in the modeled response. This noise is averaged out in the kernel calculation process and so it does not appear in the modeled response.

Table 4-2
Horizontal Cell Model Comparison

Kernels Used for Model				Dynamic MSE	Pct. Dynamic MSE
R0	H1			0.267	97.92
R0->R1	H1			0.2009	73.63
R0->R2	H1			0.1681	61.64
R0->R3	H1			0.1428	52.36
R0->R4	H1			0.1241	45.51
R0->R5	H1			0.1135	41.61
R0->R6	H1			0.1034	37.92
R0->R7	H1			0.0912	33.41
R0->R7	H1	R0	H2	0.0904	33.14
R0->R7	H1	R0->R1	H2	0.0834	30.57
R0->R7	H1	R0->R2	H2	0.0800	29.53
R0->R7	H1	R0->R3	H2	0.0778	28.51
R0->R7	H1	R0->R4	H2	0.0758	27.76
R0->R7	H1	R0->R5	H2	0.0755	27.68
R0->R7	H1	R0->R6	H2	0.0754	27.62
R0->R7	H1	R0->R7	H2	0.0758	27.77

4.3 Desensitization of Center - Flashing Surround

The stimulus used for this set of experiments was designed to indicate whether or not the cross-kernels discovered between R0 and R1 for photoreceptors in the previous experiments were due to light scatter. This stimulus desensitized the center of the receptive field by holding the central four pixels, equivalent to R0, constant at level 12. The cell was allowed to adapt to this illumination for 17 seconds. Following this adaptation period the central area was flashed from level 12 to level 15 ten times. The stimulus on time was 127.2 milliseconds and the off time was

1.3568 seconds. The surround, corresponding to R1-R7, was held constant at level 0 during this test. The cell's response to this test indicated the degree of desensitization.

For the second test the central area was held constant at level 12 and the surround , R2-R7 was flashed 10 times from level 0 to level 15. The duty cycle was the same as above. R1 was held constant at level 0. The third test was the same as the second except that the surround rest level (R2-R7) was 3 instead of 0 and the surround was flashed from level 3 to level 15. There was an 8.5 second rest period between each of the three tests.

Figures 4-10 A thru C show the results of this test for a cone photoreceptor. This was the same cell pictured in plate 4-1. This cell was not saturated by the central illumination and gave a weak hyperpolarizing response to the first test. For the second and third tests the cell showed a large depolarization.

The next three figures, 4-11 A thru C, show the results for a cell which was identified as a rod photoreceptor on the basis of the time course of its response and on its response to the first test. Figure 4-12 shows a comparison of this cell's response to the cone photoreceptor of plate 4-1. The stimulus used was a #1 spot with no background illumination and with an on time of approximately 100 milliseconds. The cone shows a rapid response to both the onset and offset of the stimulus. The rod shows a slower response to the stimulus onset and no response to the offset. Figure 4-11 A shows that this cell was saturated by

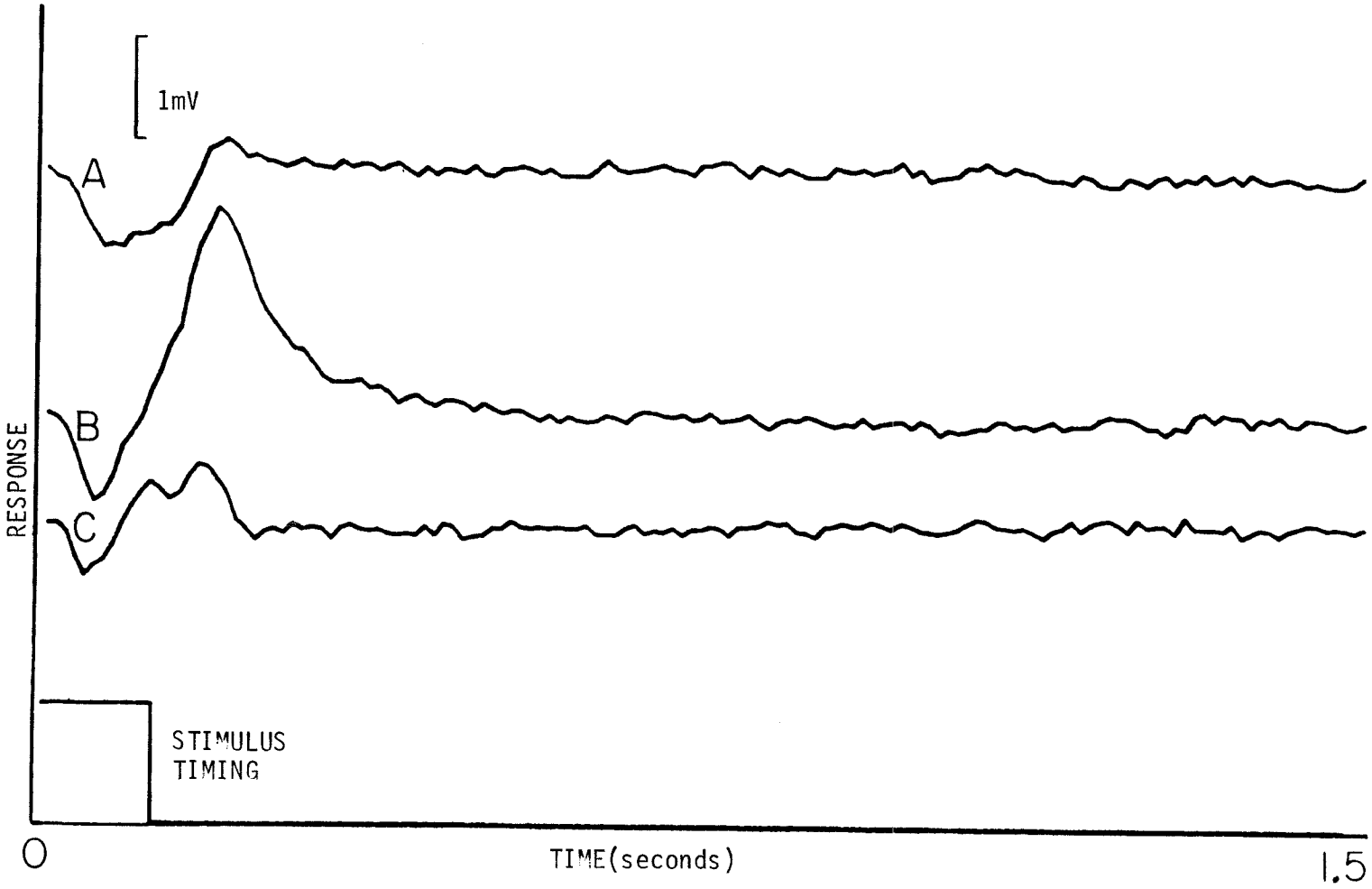

Figure 4-10 Responses of cone photoreceptor with 2 pixel by 2 pixel center at level 12.
A: Center flashed from level 12 to level 15, background steady at level 0.
B: Background flashed from level 0 to level 15, center steady at level 12.
C: Background flashed from level 3 to level 15, center steady at level 12.
The background was R2 thru R7, R1 was held at level 0 for all three cases.

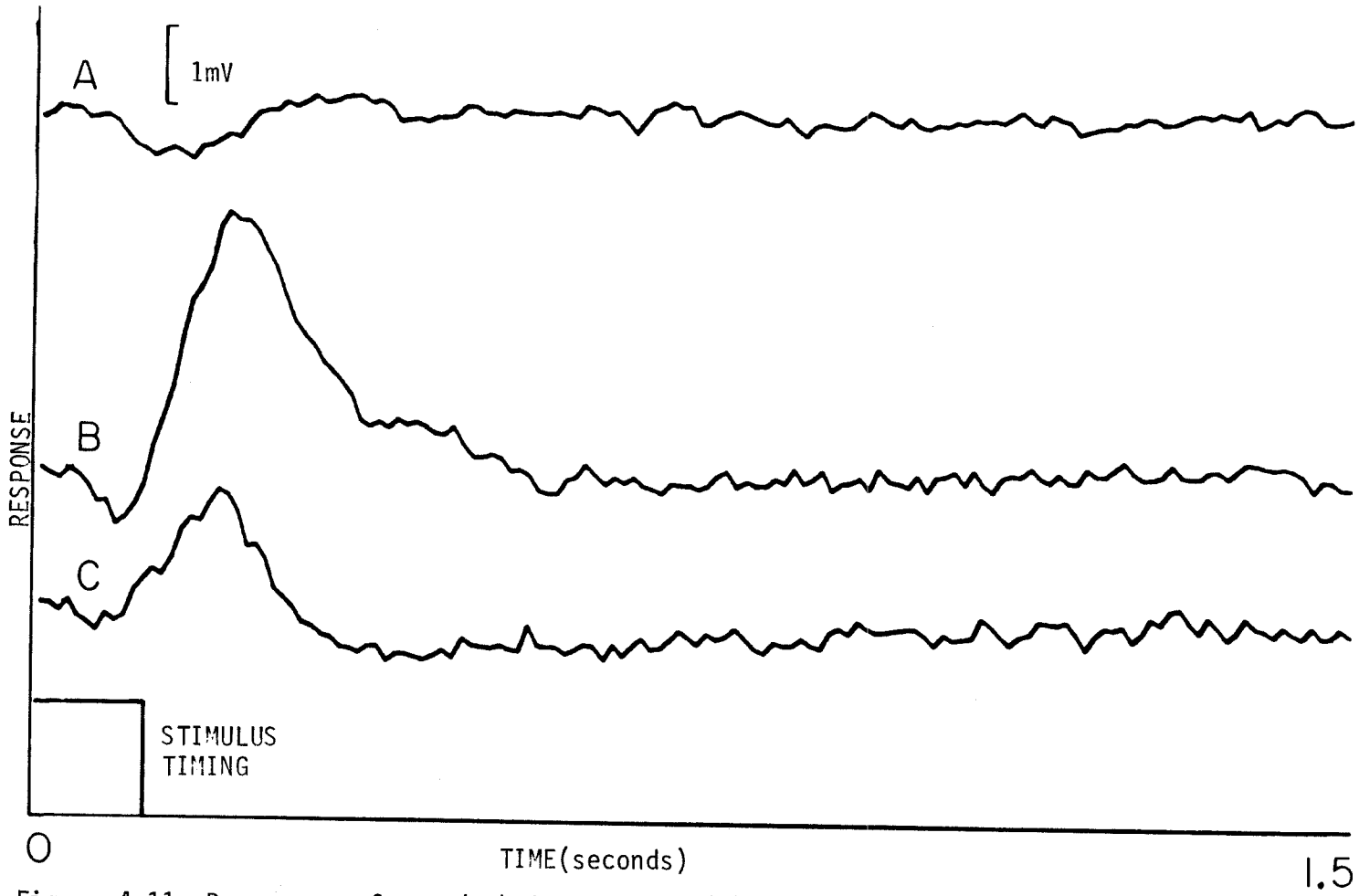

Figure 4-11 Responses of a rod photoreceptor with 2 pixel by 2 pixel center at level 12.
A: Center flashed from level 12 to level 15, background steady at level 0.
B: Background flashed from level 0 to level 15, center steady at level 12.
C: Background flashed from level 3 to level 15, center steady at level 12.
The background was R2 thru R7, R1 was held at level 0 for all three cases.

Figure 4-12 Responses from a cone photoreceptor and a rod photoreceptor to a short flash of a small spot of light. Shown are the average responses to ten stimulus presentations.

the steady illumination at level 12. It showed no response when the central area was flashed to level 15. Figures 4-11 B and 4-11 C show the same type of response as the cone.

The results of these tests for a horizontal cell are shown in the next three figures, 4-13 A thru C. The horizontal cells showed little or no response to the saturation test but showed a strong hyperpolarization to the flashing of the surround. Notice that the time of the peak of the horizontal cell hyperpolarization is just before the peak in the photoreceptor polarization.

4.4 Random Rings - Center Desensitized

The stimulus used for these experiments was a combination of the previous two stimuli. For this test the central four pixels, R0, were held constant at level 12 as in the second set of experiments. The surround, however, consisted of rings R1-R7 each independently modulated with a uniformly distributed random process as in the first experiment. This experiment was designed to study the spatial aspects of the depolarization of the photoreceptors under the conditions of the second set of experiments.

Figure 4-14 shows the first order kernels for the same cone photoreceptor as in section 4.1. Note that the kernel for R1 is biphasic, that is it has a negative peak and then a positive peak, while the rest of the nonzero kernels, R2-R4, are depolarizing. Figure 4-15 shows the receptive field plot for five experiments in cone photoreceptors. It is generated by normalizing with respect to the response per unit area in R1 since there

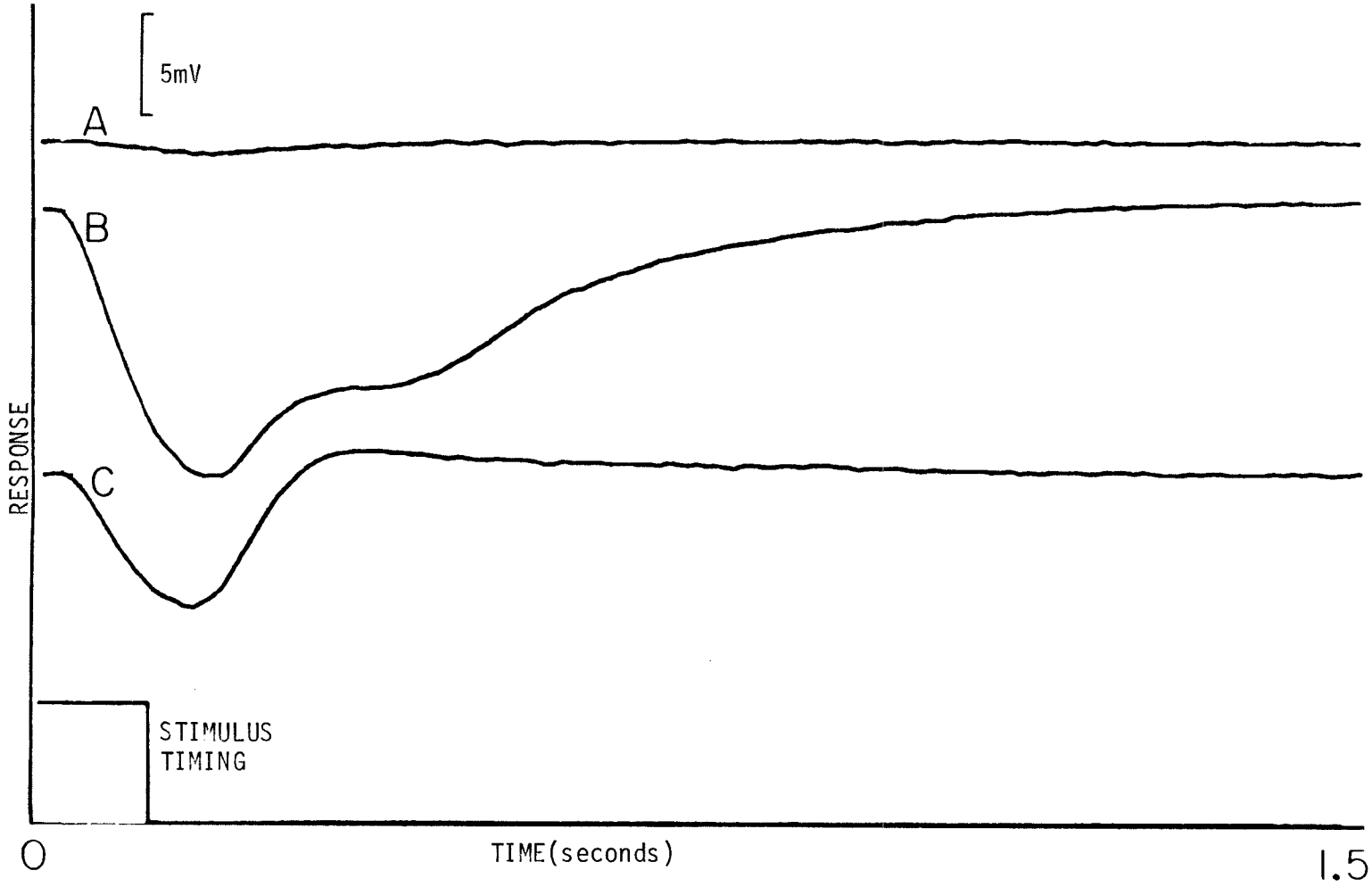

Figure 4-13 Responses of a horizontal cell with 2pixel by 2 pixel center at level 12.
A: Center flashed from level 12 to level 15, background steady at level 0.
B: Background flashed from level 0 to level 15, center steady at level 12.
C: Background flashed from level 3 to level 15, center steady at level 12.
The background was R2 thru R7, R1 was held constant at level 0 for all three cases.

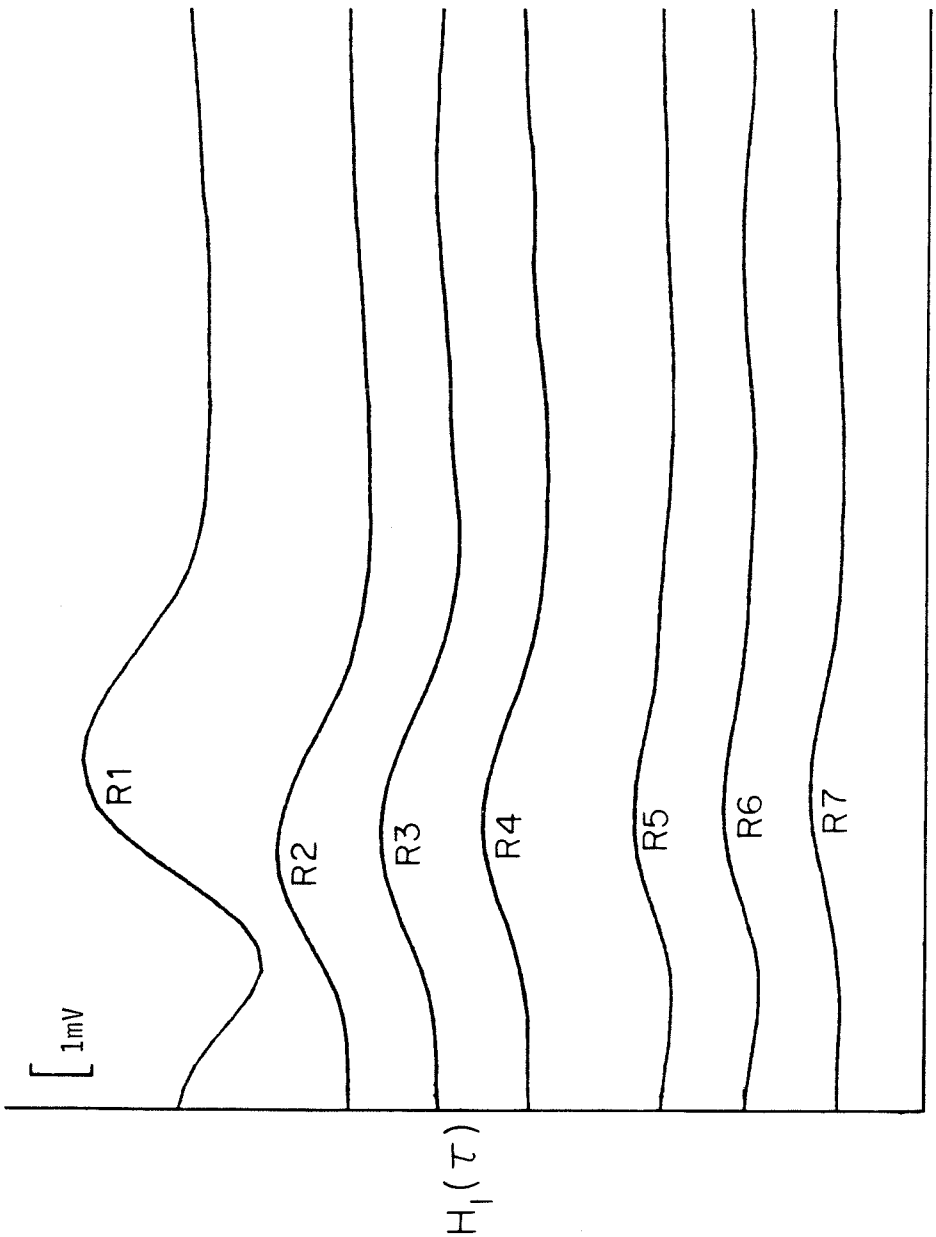

Figure 4-14 First order kernels for a cone photoreceptor. The stimulus was configured as shown in fig. 4-2. R0 was held constant at level 12. Rings R1 thru R7 were independently modulated by a 15 level uniformly distributed random signal.

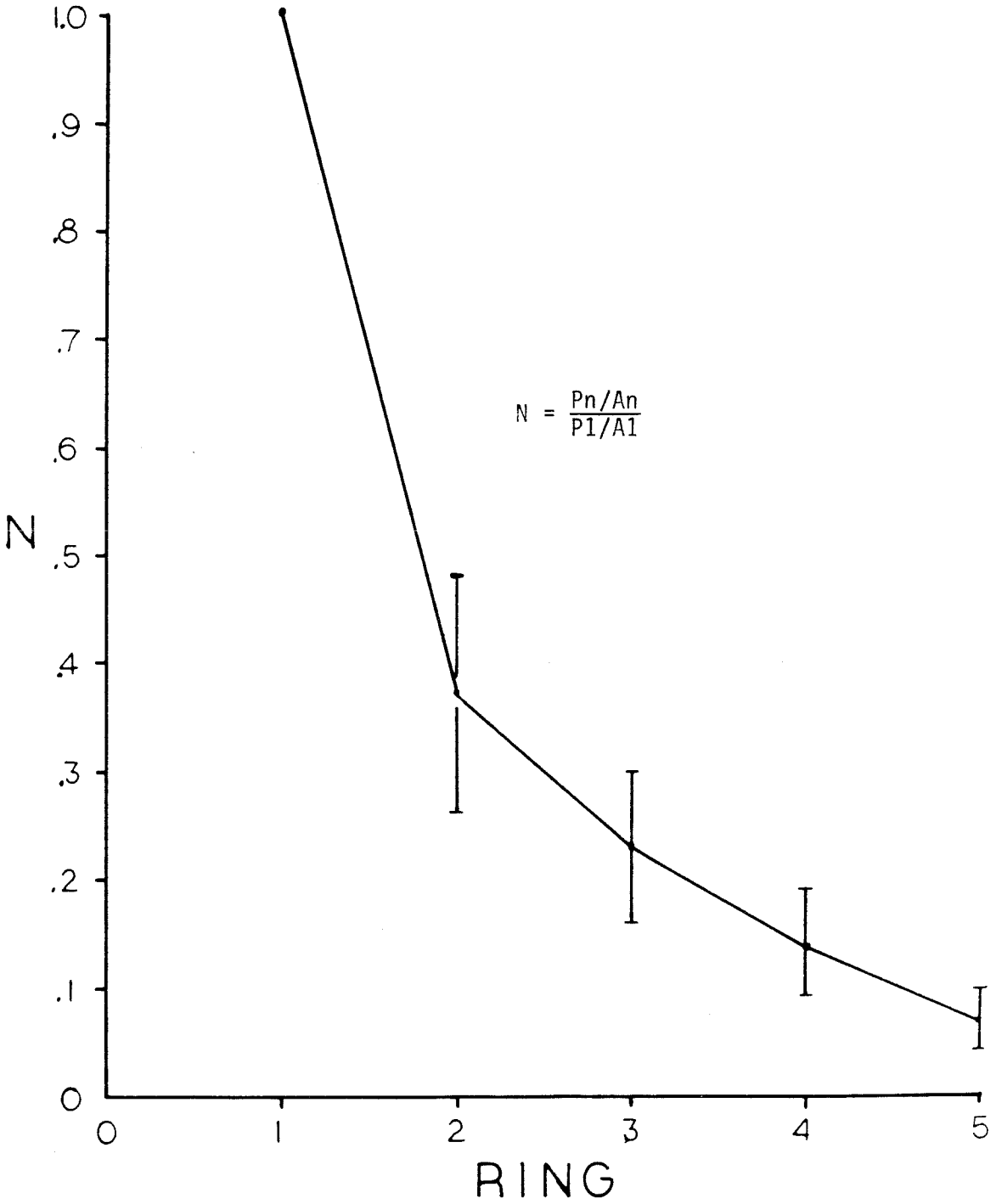

Figure 4-15 Receptive field plot for three cone photoreceptors. This plot was constructed using the peaks of the first order kernels for each of the cones. The values were averaged for each ring. The standard deviation is given by the bars. For one of the cells the experiment was repeated three times, thus there were five values in the sample. Pn is the peak of the first order kernel for ring Rn, P1 for R1. An is the area of ring Rn, A1 of R1. There is no value for ring R0 because it was held constant at level 12 for this experiment.

is no kernel for R0 in this experiment. Note that the receptive field does not fall off as rapidly under these conditions as it did for the experiments described in section 4.1.

Table 4-3 presents the results of the comparison of the modeled response and actual response for the for the cell in figure 4-14. The table shows that under these conditions the first order kernels are contributing even at ring R7. This compares to ring R1 for the experiment in section 4.2. The table also shows that the second order kernels do not improve the model significantly. This behavior is much like that of the horizontal cells studied with the random stimuli. Figure 4-16 compares the actual and modeled response to the random stimulus. It shows that the low frequency dynamics are modeled quite well. There is a lot of high frequency noise in the actual response. That noise could account for the large errors shown in table 4-3.

Table 4-3
Cone Photoreceptor Model Comparison

Kernels Used for Model				Dynamic MSE	Pct. Dynamic MSE
R1	H1			0.0605	74.01
R1->R2	H1			0.04828	59.06
R1->R3	H1			0.04139	50.63
R1->R4	H1			0.03762	46.03
R1->R5	H1			0.03611	44.17
R1->R6	H1			0.03500	42.82
R1->R7	H1			0.03388	41.44
R1->R7	H1	R1	H2	0.03347	40.94
R1->R7	H1	R1->R2	H2	0.03304	40.42
R1->R7	H1	R1->R3	H2	0.03343	40.89
R1->R7	H1	R1->R4	H2	0.03379	41.33

Figure 4-17 shows the first order kernels for the same horizontal cell as in section 4.1. Under these conditions the horizontal cell has hyperpolarizing kernels just as it did for the previous

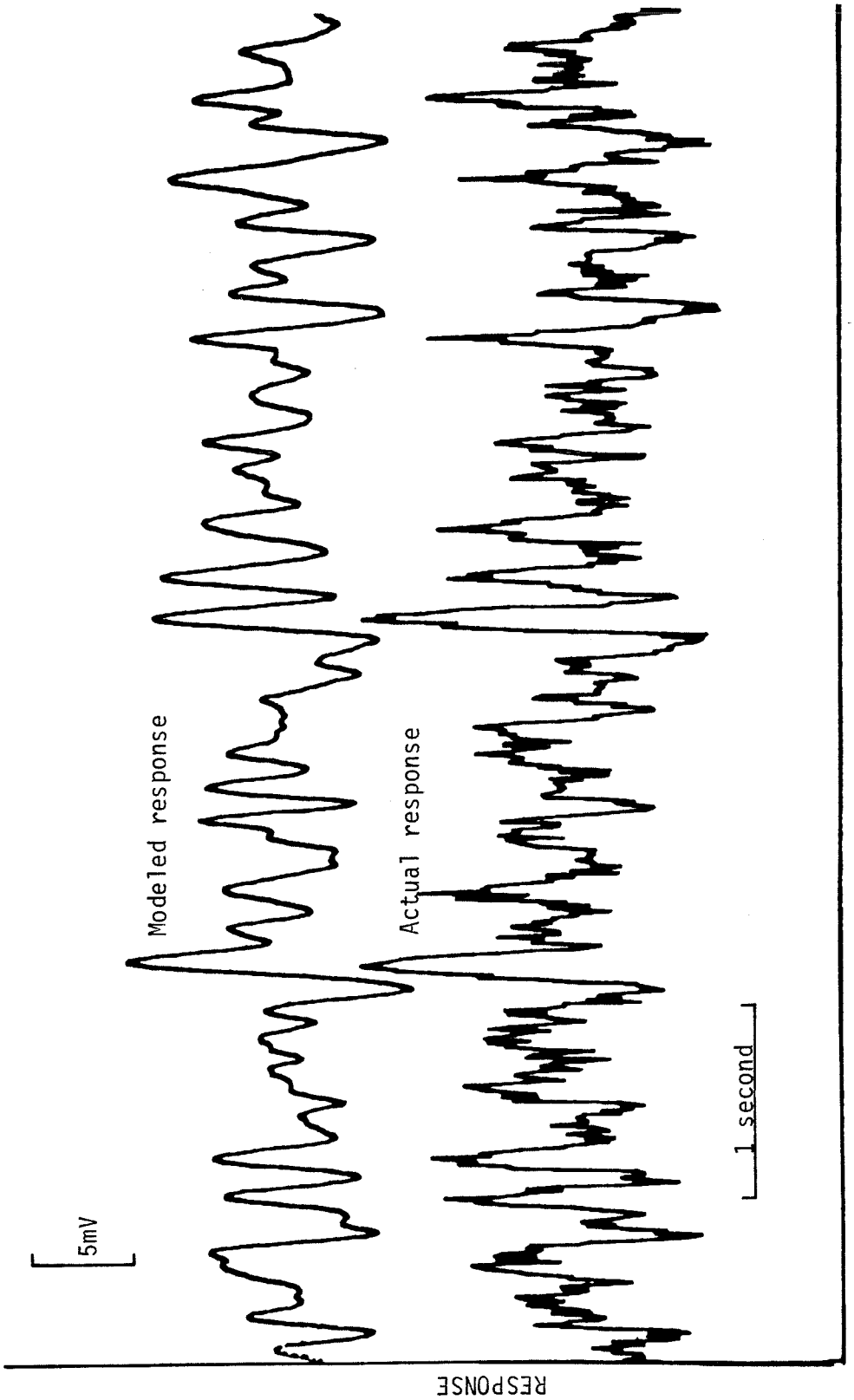

Figure 4-16 Modeled response and actual response of a cone photoreceptor to random stimuli in rings R1 thru R7 while R0 is held constant at level 12. The modeled response was computed using the kernels shown in figure 4-14.

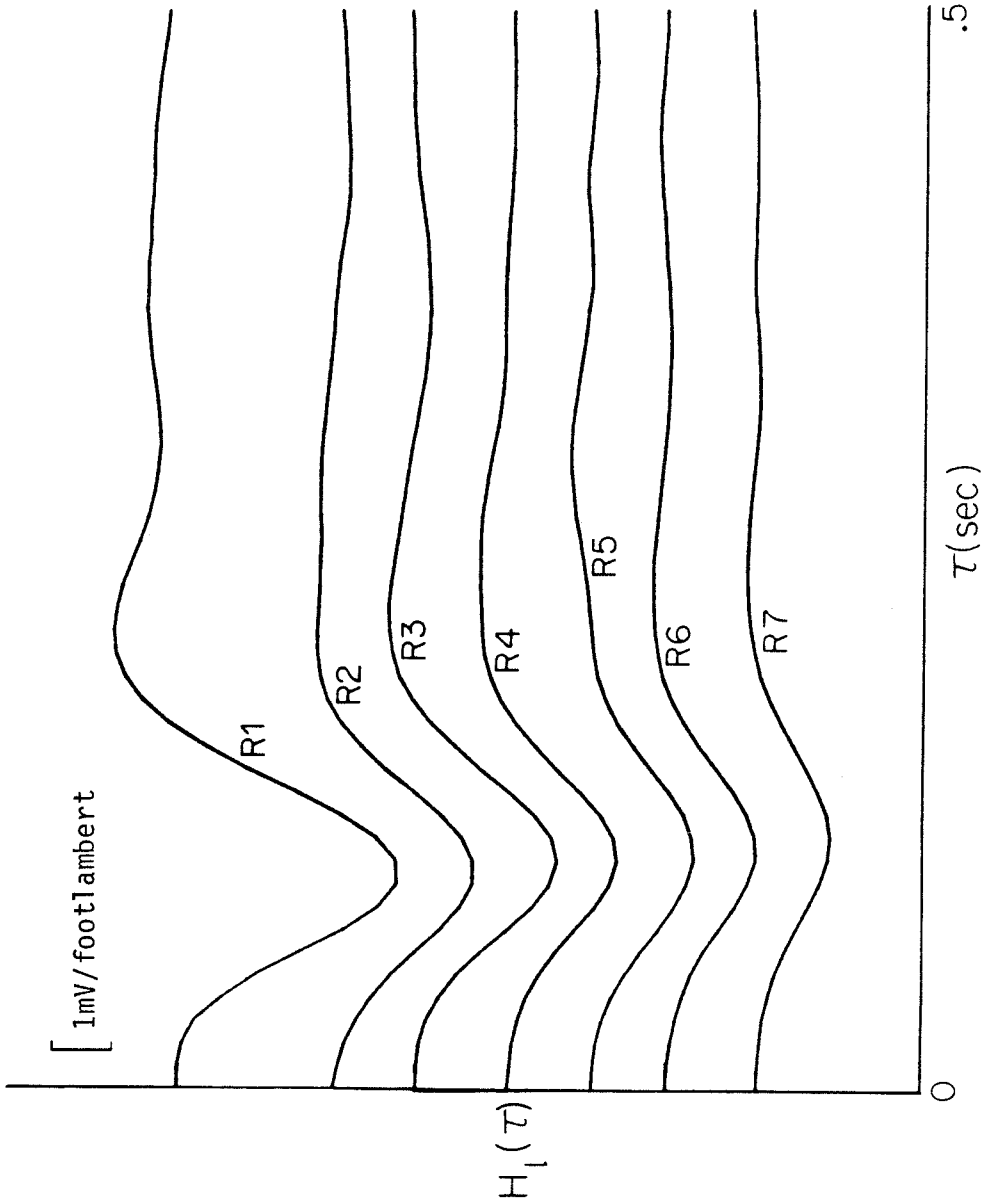

Figure 4-17 First order kernels for a horizontal cell. The stimulus was configured as shown in fig. 4-2. R0 was held constant at level 12. Rings R1 thru R7 were independently modulated by a 15 level uniformly distributed random signal.

experiments. Notice that the kernels for rings R2 thru R7 are very similar to the corresponding rings in figure 4-14 for a cone photoreceptor, but inverted. Figure 4-18 shows the receptive field plot for this cell. It is very similar to the receptive field plotted in figure 4-8 in section 4.2.

Table 4-4 shows the results of the comparison of actual and modeled responses for this cell. Consistent with the results of section 4.2 the second order kernels make very little contribution to the cells response. Figure 4-19 compares the actual and modeled response to the random stimulus. Once again, the low frequency dynamics are well modeled but the high frequency noise has been averaged out of the model.

Table 4-4
Horizontal cell model comparison

Kernels used for Model				Dynamic MSE	Pct. Dynamic MSE
R1	H1			0.2582	78.2
R1->R2	H1			0.2152	65.2
R1->R3	H1			0.1802	54.6
R1->R4	H1			0.1561	47.3
R1->R5	H1			0.1438	43.5
R1->R6	H1			0.1296	39.2
R1->R7	H1			0.1162	39.2
R1->R7	H1	R1	H2	0.1099	35.2
R1->R7	H1	R1->R2	H2	0.1057	32.0
R1->R7	H1	R1->R3	H2	0.1032	31.3
R1->R7	H1	R1->R4	H2	0.1028	31.1
R1->R7	H1	R1->R5	H2	0.1027	31.1

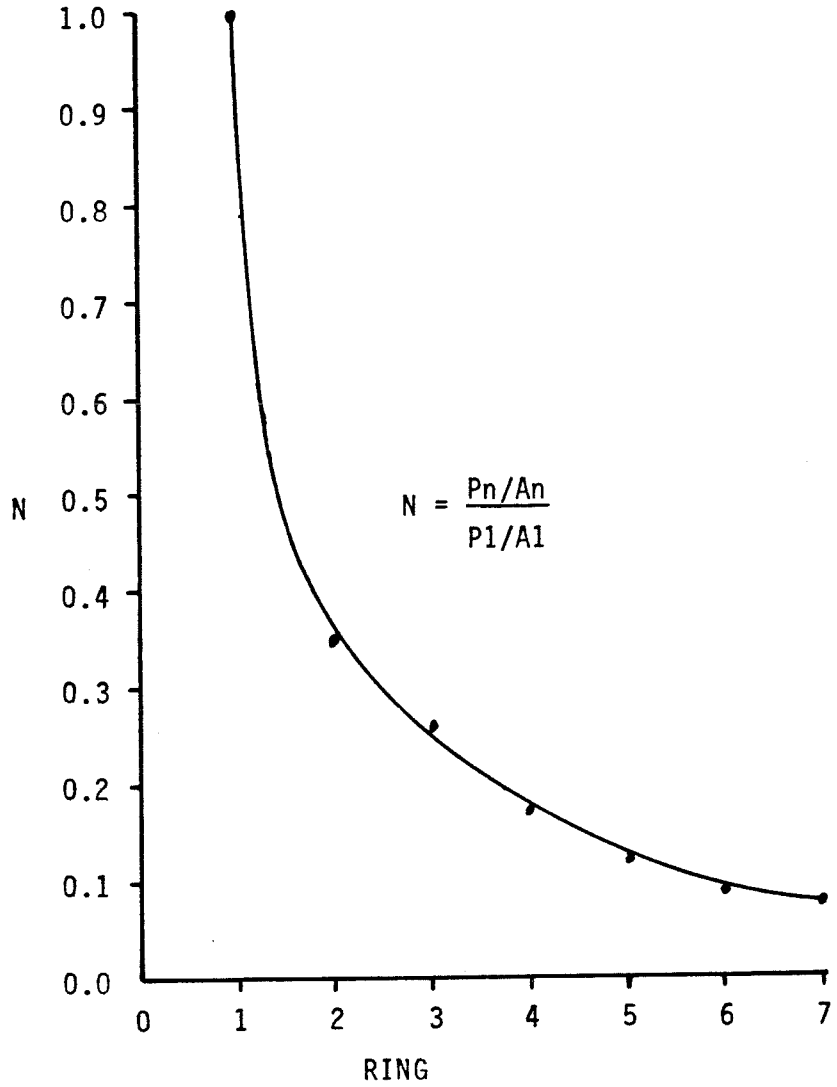

Figure 4-18 Receptive field plot for horizontal cell. This plot was constructed using the first order kernels shown in fig. 4-17. Pn is the peak of the first order kernel for ring Rn, P1 for R1. An is the area of ring Rn, A1 of R1. There is no value for ring R0 because it was held constant at level 12 for this experiment.

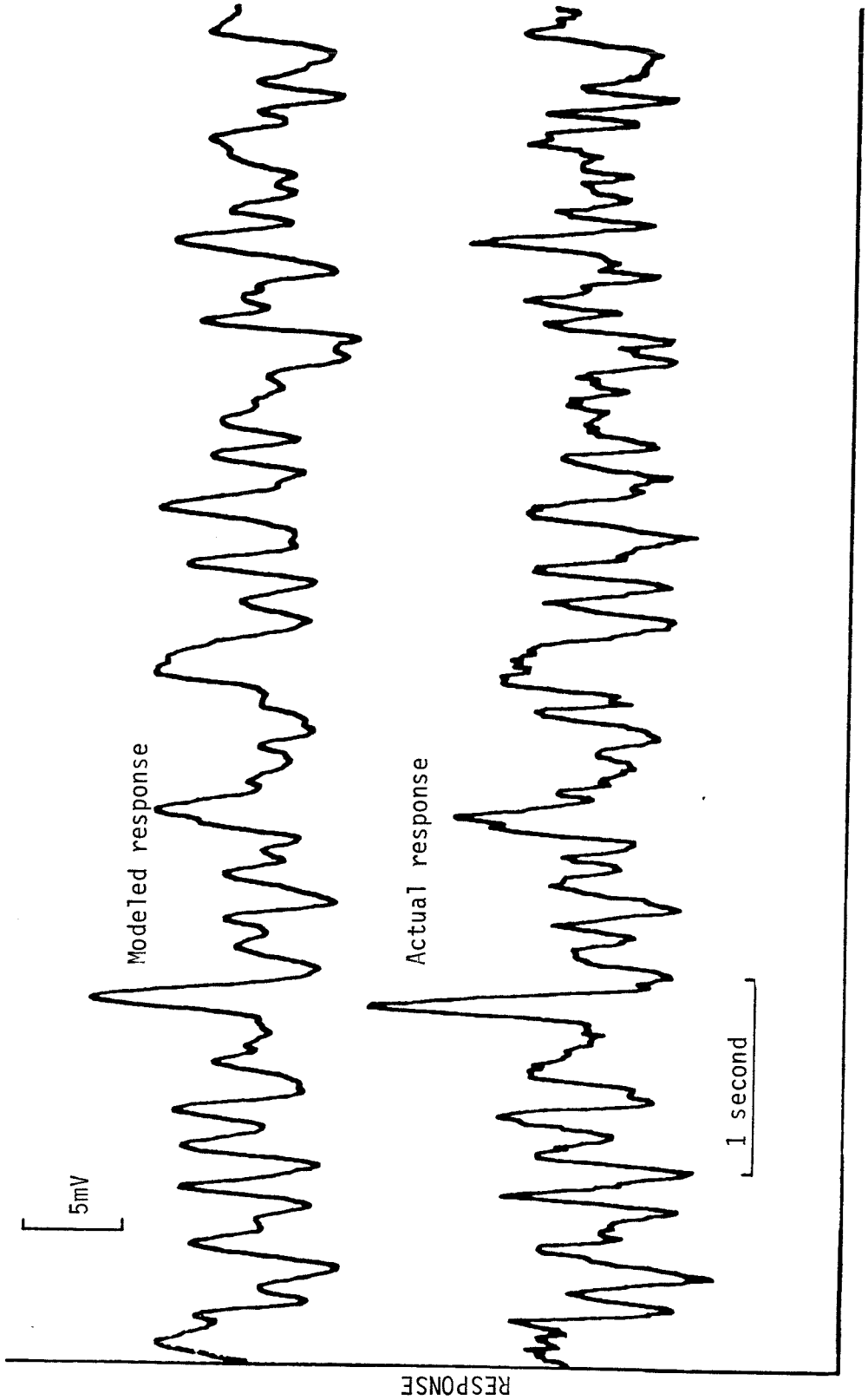

Figure 4-19 Modeled response and actual response of a horizontal cell to random stimuli in rings R1 thru R7 while R0 is held constant at level 0. The modeled response was computed using the kernels shown in figure 4-17.

5. DISCUSSION

Previous studies have proven the existence of functional feedback from the horizontal cells to the photoreceptors. This has been shown by two electrode experiments in the turtle retina [6] and has been indicated in single electrode experiments [34] and morphological studies [23,77,79]. The existence of this feedback arrangement has led to postulates that horizontal cells provide a pathway coupling different types of cones in multi-cone retinas and that this coupling in turn causes C-type horizontal cell responses [34]. It has also led to postulates that horizontal cells mediate the bipolar cell surround via the cones. Polarization of bipolar cells by current injection in nearby horizontal cells has given support to this hypothesis [84].

Finally, it has been postulated that horizontal cells pool information about the average level of illumination over large areas of the retina. One study on the effect of surround illumination on the sensitivity of bipolar cell center supports this hypothesis [80]. This study did not indicate the pathway for the surround to center interaction.

Combining the existence of horizontal cell feedback to photoreceptors with the idea of a pooling of information about average illumination suggests the pathway might be via the photoreceptors. The experiments described in the previous chapter were designed to test that very hypothesis; that photoreceptor sensitivity would be altered by illumination of the seemingly nonfunc-

tional surround of the photoreceptor receptive field.

The results of the experiments described in section 4.2 give the strongest support for this hypothesis. Visual stimulation of photoreceptors with a pattern of randomly modulated rings consistently showed the existence of a cross kernel between the center, R0, and the nearest ring, R1, which predicted a sensitivity change in R0 due to the illumination in R1.

To further clarify the influence of the surround on the photoreceptor in the center the response of the photoreceptor to steady illumination in R1 and a sensitivity test stimulus in R0 was modeled using the self kernels for R0 and the R0xR1 cross kernel. The sensitivity test stimulus is nominally at level 7. It represents a time series of flashes of dark and light from level 7 to each of the other levels 0 to 14. Figure 5-1 presents the intensity response curves for the modeled response. It was constructed by plotting the peak response to each level of the sensitivity test stimulus versus the intensity of that level in log-footlamberts. Curve A shows the result for R1 at level 0, curve B for R1 at level 7 and curve C for R1 at level 14. These curves clearly show that the response of the photoreceptor is compressed by surround illumination.

The results of this modeling support the results described in section 4.1. A comparison of figures 4-1 and 5-1 shows that the modeled results are much clearer than the experimental results. There are at least two reasons why the modeled results

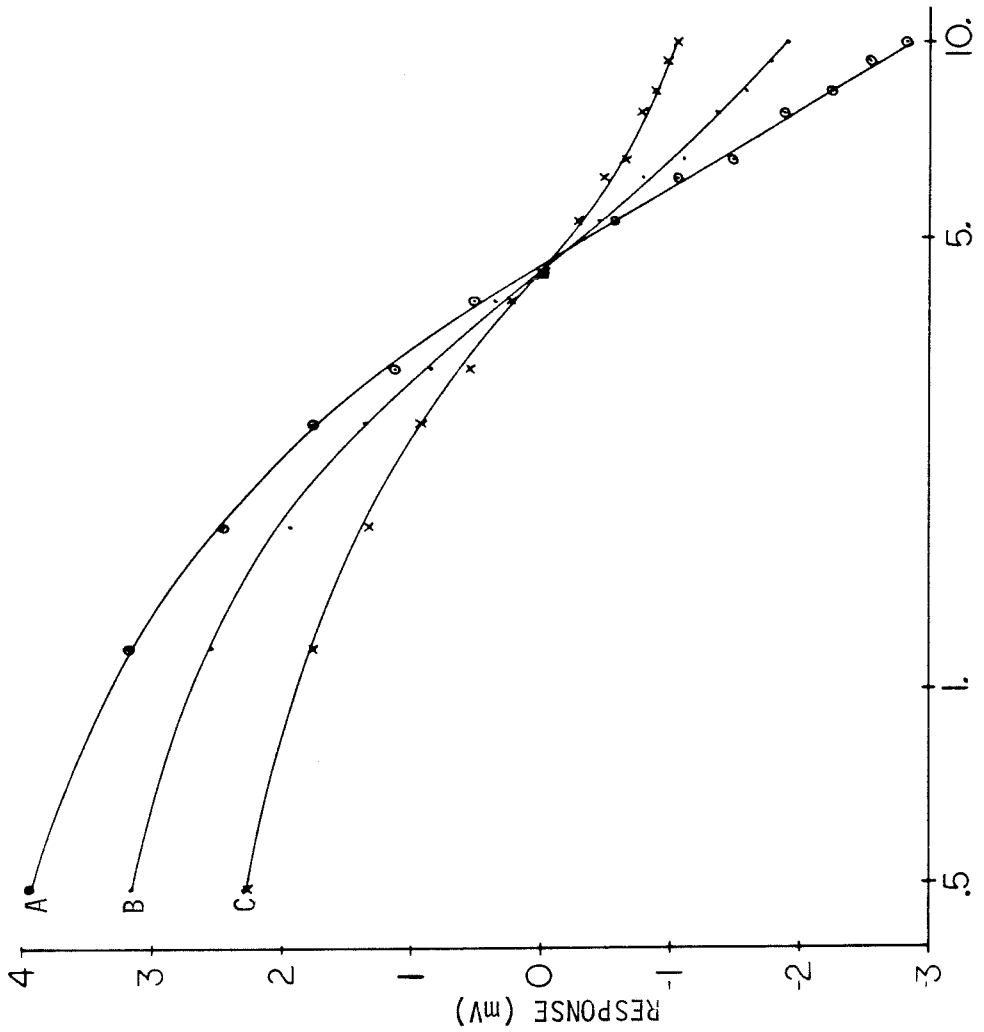

Figure 5-1 Intensity-response curves for a cone photoreceptor. Calculated using the first and second order kernels for ring R0 and the cross kernel between R0 and R1. R1 was constant at level 0 (A), 7 (B), and 14 (C). R0 was flashed from level 7 to each other level.

are clearer. The first reason is that the test conditions were not identical for the two cases. Recall that in the experiment of section 4.1 the sensitivity was measured under the conditions background level 0 and center level 0 (BG0CT0), BG0CT3 and BG3CT3. A change in level of 0 to 3 should not be expected to give as striking a result as a change from 0 to 7 to 14.

The second reason has to do with the efficiency of the random stimulus in characterizing the properties of a system. The random stimulus effectively tests the response of the system to thousands of combinations of stimulus configuration. To obtain similar results with a conventional stimulus, such as the one in experiment 4.1, an average response would have to be developed for several thousand stimulus presentations for each stimulus configuration. Presentation of the sensitivity test stimulus requires 24 seconds for one pass from level 0 to level 15. To test each of the three configurations 1000 times would thus require 72,000 seconds or a 20 hour experiment. The random stimulus was able to provide the data for a general characterization of the system in a 5 minute experiment.

One question that comes to mind is whether it can be shown that the response compression is not due to light scatter from surround to center. An experimental or an analytical approach may be taken in dealing with this problem. A discussion of the results of sections 4.3 and 4.4 will present the experimental answer but first let us consider the analytical approach.

Consider a system with two inputs x(t) and u(t) and first and second order self kernels for both inputs but no cross kernel between them. We may now write the functional representation of the system as:

$$y(t) = \sum_{\tau=0}^{M} h_{1_x}(\tau)x(t-\tau) + \sum_{\tau=0}^{M} h_{1_u}(\tau)u(t-\tau)$$

$$+ \sum_{\tau_1=0}^{M}\sum_{\tau_2=0}^{M} h_{2_x}(\tau_1,\tau_2)x(t-\tau_1)x(t-\tau_2) \qquad (1)$$

$$+ \sum_{\tau_1=0}^{M}\sum_{\tau_2=0}^{M} h_{2_u}(\tau_1,\tau_2)u(t-\tau_1)u(t-\tau_2)$$

Now consider what happens if there is scatter from u(t) to x(t). In this case we may rewrite the input x(t) as $x'(t) = x(t) + su(t)$ where s is the fraction of scatter. Substituting x'(t) into equation (1) we have:

$$y(t) = \sum_{\tau=0}^{M} h_{1_x}(\tau)[x(t-\tau) + su(t-\tau)]$$

$$+ \sum_{\tau=0}^{M} h_{1_u}(\tau)u(t-\tau)$$

$$+ \sum_{\tau_1=0}^{M}\sum_{\tau_2=0}^{M} h_{2_x}(\tau_1,\tau_2)[x(t-\tau_1) + su(t-\tau_1)][x(t-\tau_2) + su(t-\tau_2)]$$

$$+ \sum_{\tau_1=0}^{M}\sum_{\tau_2=0}^{M} h_{2_u}(\tau_1,\tau_2)u(t-\tau_1)u(t-\tau_2)$$

Collecting terms we have:

$$y(t) = \sum_{\tau=0}^{M} h_{1_x}(\tau)x(t-\tau) + \sum_{\tau=0}^{M}[h_{1_u}(\tau) + sh_{1_x}(\tau)]u(t-\tau)$$

$$+ \sum_{\tau_1=0}^{M}\sum_{\tau_2=0}^{M} h_{2_x}(\tau_1,\tau_2)x(t-\tau_1)x(t-\tau_2)$$

$$+ \sum_{\tau_1=0}^{M}\sum_{\tau_2=0}^{M} [h_{2_u}(\tau_1,\tau_2) + sh_{2_x}(\tau_1,\tau_2)]u(t-\tau_1)u(t-\tau_2)$$

$$+ 2s\sum_{\tau_1=0}^{M}\sum_{\tau_2=0}^{M} h_{2_x}(\tau_1,\tau_2)x(t-\tau_1)u(t-\tau_2) \qquad (2)$$

Examining equation (3) we see that the first and second order kernels that would be calculated for the input u(t) would be corrupted by the kernels for the input x(t). More importantly, though, the fifth term indicates that we would now see something if we calculated the cross kernel between x and u whereas with no scatter there would have been no cross kernel. What is important to note is that the cross kernel would be the second order kernel for the input x(t) multiplied by twice the scatter factor s.

Figures 4-5 A and B show the self and cross kernels for area R0 from the random rings experiment of section 4.2. A comparison of these figures shows that there are few if any similarities between the two kernels. Based on the analysis just presented it appears that the cross kernel is not due to light scatter from surround to center. Thus the modeled results presented in figure 5-1 indicate a neural interaction between the horizontal cells that surround the photoreceptor and the receptor itself.

As was mentioned previously the experiments of sections 4.3 and 4.4 were designed to minimize the effects of light scatter and look for neural interaction between the horizontal cell dominated surround and the photoreceptor dominated center. The experiment described in section 4.3 was similar to one used by Baylor, Fuortes and O'Bryan (1971) to study the receptive fields of cones in the turtle retina. The results presented in section 4.3 agree well with their results.

The basic scheme of the experiment was to desensitize the photoreceptor in the center of the receptive field so that the effect of any scattered light would be eliminated or at least reduced. This desensitization was accomplished by holding the central four pixels constant at level 12. They covered a square area just over 180 microns wide. For good measure a one pixel wide 'buffer zone' around the center 4 pixels was held at level 0. The buffer zone increased the distance from the surround illumination to the center and and therefore reduced the amount of scattered light. The surround was flashed 10 times from level 0 to level 15 and then 10 more times from level 3 to level 15. The results presented in figure 4-10 for a cone and 4-11 for a rod clearly indicate a neural interaction. Curve A in each figure shows the average response when the center was flashed from level 12 to level 15 10 times. It indicates that any scattered light should have produced a hyperpolarization of the receptor instead of the depolarization that occurred. Figure 4-13 shows that the peak of the horizontal cell hyperpolarization for this

experiment coincides with the peak of the photoreceptor depolarization. This is good evidence that horizontal cell feedback is causing the depolarization through an inverting synapse of some type.

This result is consistent with the hypothesis of response compression in a photoreceptor by illumination of the surround. It also indicates that as in other species there is negative feedback from horizontal cells to cones. It is the first physiological evidence I am aware of that there is also negative feedback from horizontal cells to rods.

The final set of results to be discussed is that of section 4.4. The stimulus used for these experiments was a combination of center desensitization and randomly modulated rings. The results of this section are in good agreement with those of the previous sections and those of Baylor, Fuortes and O'Bryan (1971). They found that with the center illuminated stimulation of the near surround of a cone gave a hyperpolarizing response. As is shown in figure 4-14 the first order kernel for R1 is biphasic. This indicates that ring R1 covered the transition zone between receptor-receptor coupling and horizontal cell feedback. The kernels for the rest of the rings, R2-R7, are seen to be purely depolarizing. One surprising thing about these results is their spatial extent. The kernels are clearly visible clear out to R7. This is a definite indication of horizontal cell involvement.

The experiments that have been discussed were all performed on horizontal cells as well as photoreceptors. One clear distinction between the two types of neurons was given by the results of the random rings experiment with no center desensitization. Figures 4-4 and 4-8 show the receptive field plots that were constructed from the first order kernel peaks for a cone and a horizontal cell respectively. The horizontal cell receptive field spreads as far as R6 and possibly a little farther while the cone receptive field is entirely within R0. Thus the horizontal cells are indicated by the results of section 4.4 to be the mediators of the receptor surround.

Further support for this is gained by comparing the horizontal cell kernels from section 4.4 with the receptor kernels. Note that the horizontal cell kernels for R2 thru R7 are very similar to the corresponding receptor kernels if their polarity is reversed.

In this dissertation I have presented the results of intracellular recordings from photoreceptors and horizontal cells in the retina of the frog, R. pipiens. These results have supported the results of investigations in the retinas of other vertebrate species. Specifically they have supported the idea of horizontal cell feedback to cone photoreceptors. They have expanded that idea by supporting the hypothesis of photoreceptor response compression by surround illumination. They have also extended the idea of horizontal cell feedback to include rod photoreceptors. Taken together with the results of Thibos and Werblin

(1978) on response compression of bipolar cell centers by surround illumination they lend support to the idea of bipolar cell surround mediation by horizontal cells via the photoreceptors.

I believe it is fair to say that the results obtained using conventional stimuli, that is the results of of sections 4.1 and 4.3, were greatly enhanced if not overshadowed by the results obtained using randomly modulated stimuli. This is an illustration of the efficiency of the nonparametric nonlinear system identification technique. It is my hope that by continuing to develop this technique from the discrete domain, considering that it will be implemented on a digital computer, it will be more widely used. I believe that it has potential in adaptive control and could also be useful in nondestructive testing. It is a powerful technique and I think it will serve us well as we work with it and develop a better understanding of how to exploit it.

References

[1] Azuma, M. and Azuma, K. The increase in sensitivity following light illumination in frog photoreceptors. Vision Res. (1979), 19, pp.1171-1175

[2] Barrman, Ch. and Scheibner, H. The dark adaptation of single units in the isolated frog retina following partial bleaching of rhodopsin. Vision Res. (1968), 8, pp.1127-1138

[3] Barth, L. G. Embryology, Dreyden Press,1953

[4] Bastian, B. L. and Fain, G. L. Light adaptation in toad rods: requirement for an internal messenger which is not calcium. J. Physiol. (1979), 297, pp. 493-520

[5] Baylor, D. A. and Fuortes, M. G. F. Electrical response of single cones in the retina of the turtle. J. Physiol. (1970), 207, pp.77-92

[6] Baylor, D. A., Fuortes, M. G. F. and O'Bryan, P. M. Receptive fields of cones in the retina of the turtle. J. Physiol. (1971), 214, pp.265-294

[7] Baylor, D. A. and Hodgkin, A. L. Changes in time scale and sensitivity in turtle photoreceptors. J. Physiol. (1974), 242, pp.729-758

[8] Baylor, D. A., Hodgkin, A. L. and Lamb, T. D. Reconstruction of the electrical responses of turtle cones to flashes and steps of light. J. Physiol. (1974), 242, pp.759-791

[9] Baylor, D. A. and Hodgkin, A. L. Detection and resolution of visual stimuli by turtle photoreceptors. J. Physiol. (1973), 234, pp.163-198

[10] Boynton, R. M. and Whitten, D. N. Visual adaptation in monkey cones: recordings of late receptor potentials. Science (1970), 170, pp.1423-1426

[11] Byzov, A. L. Origin of non-linearity of voltage-current relationships of turtle cones. Vision Res. (1979), 19, pp.469-477

[12] Cervetto, L. and Fuortes, M.G.F. Excitation and interaction in the retina. Ann. Rev. Bioph. Bioeng. (1978) 7 pp.229-251

[13] Cervetto, L., Pasino, E. and Torre, V. Electrical responses of rods in the retina of Bufo marinus. J. Physiol. (1977), 267, pp.17-51

[14] Cervetto, L., Torre, V. and Cepovilla, M. Mechanisms of generation of signals in vertebrate photoreceptors. Sensory Processes (1978), 2, pp.316-320

[15] Copenhagen, D. R. and Owen, W. G. Coupling between rod photoreceptors in a vertebrate retina. Nature (1976), 260, pp.57-59

[16] Copenhagen, D. R. and Owen, W. G. Functional characteristics of lateral interactions between rods in the retina of the snapping turtle. J. Physiol. (1976), 259, pp.251-282

[17] Dawis, S. M. Light adaptation in cone photoreceptors: the occurence and significance of unitary adaptive strength. Biol. Cybernetics (1978), 34, pp.35-41

[18] Detwiler, P. B., Hodgkin, A. L. and McNaughton, P. A. A surprising property of electrical spread in the network of rods in the turtles retina. Nature (1978), 274, pp.562-565

[19] Detwiler, P. B., and Hodgkin, A. L. Electrical coupling between cones in turtle retina. J. Physiol. (1979), 291, pp.75-100

[20] Detwiler, P. B., Hodgkin, A. L., and McNaughton, P. A. Temporal and spatial characteristics of the voltage response of rods in the retina of the snapping turtle. J. Physiol. (1980), 300, pp.213-250

[21] Donner, K. O. and Reuter, T. Visual pigments and photoreceptor function. Frog Neurobiology A Handbook, Ed. R. Llinas and W. Precht, Springer-Verlag,1976

[22] Dowling, J. E. Neural and photochemical mechanisms of visual adaptation in the rat. J. Gen. Physiol. (1963), 46, pp.1287-1301

[23] Dowling, J. E. Synaptic organization of the frog retina: an electron microscopic analysis comparing the retinas of frogs and primates. Proc. Royal Soc. Lond. B. (1968), 170, pp.205-228

[24] Dowling, J. E. Information processing by local circuits: the vertebrate retina as a model system. The Neurosciences: Fourth Study Program. Ed. F. O. Schmitt, MIT Press, Cambridge, Mass.,1979

[25] Dowling, J. E. and Boycott B. B. Organization of the primate retina: electron microscopy. Proc. R. Soc. London, Ser. B (1966), 166, pp.80-111

[26] Dowling, J. E. and Ripps, H. Adaptation in skate photoreceptors. J. Gen. Physiol. (1972), 60, pp.698-719

[27] Dowling J. E. and Ripps, H. S-potentials in the skate retina: Intracellular recordings during light and dark adaptation. J. Gen. Physiol. (1971), 58, pp.163-189

[28] Ernst, W. and Kemp, L. M. Reversal of photoreceptor bleaching and adaptation by microsecond flashes. Vision Res. (1979), 19, pp.363-365

[29] Evans, E. M. On the ultrastructure of the synaptic region of visual receptors in certain vertebrates. Z. Zellforsch. Mikrosk. Anat. (1976), 71,pp.499-516

[30] Fain, G. L. Sensitivity of toad rods: Dependence on wavelength and background illumination. J. Physiol. (1976), 261, pp.71-101

[31] Fain, G. L., Gold, G. H. and Dowling, J. E. Receptor coupling in the toad retina. Cold Spring Harbor Symp. Quant. Biol. (1975), 40 pp.547-561

[32] Flaming, D. G. and Brown, K. T. Effects of calcium on the intensity response curve of toad rods. Nature (1979), 278, pp.852-853

[33] Fuortes, M.G.F. Responses of cones and horizontal cells in the retina of the turtle. Invest. Opthalmology (1972), 11, pp.275-284

[34] Fuortes, M.G.F. and Simon, E. J. Interactions leading to horizontal cell responses in the retina of the turtle. J. Physiol. (1974), 240, pp.177-198

[35] Gerschenfeld, H. M. and Piccolino, M. Muscarine antagonists block cone to horizontal cell transmission in the turtle retina. Nature (1977), 268, pp.257-259

[36] Gold, G. H. Photoreceptor coupling in retina of the toad, Bufo marinus. II. Physiology. J. Neurophysiol. (1979), 42, pp.311-328

[37] Grusser, O.-J. Cat ganglion-cell receptive fields and the role of horizontal cells in their generation. The Neurosciences: Fourth Study Program. Ed. F. O. Schmitt, MIT Press, Cambridge, Mass.,1979

[38] Hagins, W. A. Excitation in vertebrate photoreceptors. The Neurosciences: Fourth Study Program. Ed. F. O. Schmitt, MIT Press, Cambridge, Mass.,1979

[39] Hanani, M. and Vallerga, S. Rod and cone signals in the horizontal cells of the tiger salamander retina. J. Physiol. (1980), 298, pp. 397-405

[40] Jordan, C. Calculus of Finite Differences, Chelsea, New York, 1965.

[41] Kaneko, A. Physiological and morphological identification of horizontal, bipolar and amacrine cells in goldfish retina. J. Physiol. (1970), 207 pp.623-633

[42] Kaneko, A. Electrical connections between horizontal cells in the dogfish retina. J. Physiol. (1971), 213, pp.95-105

[43] Kleinschmidt, J. and Dowling, J. E. Intracellular recordings from gecko photoreceptors during light and dark adaptation. J. Gen. Physiol. (1975), 66, pp.617-648

[44] Kroeker, J. P. Wiener analysis of nonlinear systems using Poisson-Charlier crosscorrelation. Biol. Cybernetics (1977), 27, pp.221-227

[45] Kroeker, J. P. Synaptic facilitation in Aplysia explored by random presynaptic stimulation. J. Gen. Physiol. (1979), 73, pp.747-763

[46] Kroeker, J. P. Wiener analysis of functionals of a Markov chain: Application to neural transformations of random signals. Biol. Cybernetics (1980), 36, pp.243-248

[47] Lamb, T. D. Spatial properties of horizontal cell responses in the turtle retina. J. Physiol. (1976), 263, pp.239-255

[48] Lamb, T. D., Baylor, D. A. and Yau, K.-W. The membrane current of single rod outer segments. Vision Res. (1979), 19, pp.385

[49] Lamb, T. D. and Simon, E. J. The relation between intercellular coupling and electrical noise in turtle photoreceptors. J. Physiol. (1976), 263, pp.257-286

[50] Lasansky, A. Interactions between horizontal cells of the salamander retina. Invest. Opthalmology (1976), 15, pp.909-916

[51] Lasansky, A. and Vallerga, S. Horizontal cell responses in the retina of the larval tiger salamander. J. Physiol. (1975), 251, pp.145-165

[52] Marchiafava, F. L. Horizontal cells influence membrane potential of bipolar cells in the retina of the turtle. Nature (1978), 275, pp.141-142

[53] Marmarelis, P. Z. and McCann, G. D. Development and application of white-noise modeling techniques for studies of insect visual nervous systems. Kybernetik (1973),

12,pp.74-89

[54] Marmarelis, P. Z. and Naka, K.-I. White-noise analysis of a neuron chain: An application of the Wiener theory. Science (1972), 175, pp. 1276-1278

[55] Marmarelis, P. Z. and Naka, K.-I. Spatial distribution of potential in a flat cell, application to the catfish horizontal cell layers. Biophysical Journal (1972), 12, pp.1515-1532

[56] Marmarelis, P. Z. and Naka, K.-I. Experimental analysis of a neural system: Two modeling approaches. Kybernetik (1974), 15,pp.11-26

[57] Marmarelis, P. Z. and Naka, K.-I. Identification of multi-input biological systems. IEEE Trans. on Biomedical Engineering (1974), BME-21, pp.88-101

[58] Marshall, L. M. and Werblin, F. S. Synaptic transmission to the horizontal cells in the retina of the larval tiger salamander. J. Physiol. (1978), 279, pp.321-364

[59] Matsumoto, N. and Naka, K.-I. Identification of intracellular responses in the frog retina. Brain Res. (1972), 42, pp.59-71

[60] Missotten, L. The Ultrastructure of the Retina, Brussels: Arscia Uitgaven N.V.,1965

[61] Mooney, R. D. GABA and the lateral spread of tonic activity in the frog retina. Vision Res. (1979), 19, pp.501-505

[62] Naka, K.-I. The horizontal cells. Vision Res. (1972), 12, pp.573-578

[63] Naka, K.-I. and Rushton, W. A. H. The generation and spread of S-potentials in fish (Cyprinidae). J. Physiol. (1967), 192, pp.437-461

[64] Naka, K.-I. and Nye, P. W. Role of horizontal cells in organization of the catfish retinal receptive field. J. Neurophysiol. (1971), 34, pp.785-801

[65] Normann, R. A. and Perlman, I. The effects of background illumination on the photoresponses of red and green cones. J. Physiol. (1979), 286, pp.491-507

[66] Normann, R. A. and Perlman, I. Signal transmission from red cones to horizontal cells in the turtle retina. J. Physiol. (1979), 286, pp.509-524

[67] Normann, R. A. and Perlman, I. Evaluating sensitivity changing mechanisms in light adapted photoreceptors. Vision Res. (1979), 19, pp.391-394

[68] Normann, R. A. and Pochobradsky, J. Oscillations in rod and horizontal cell potential: Evidence for feedback to rods in the vertebrate retina. J. Physiol. (1976), 261, pp.15-29

[69] Normann, R. A. and Werblin, F. S. Control of retinal sensitivity: I. Light and dark adaptation of vertebrate rods and cones. J. Gen. Physiol. (1974), 63, pp.37-61

[70] Ogden, T., Citron, M., Melton, R., McCann, G., and Pierantoni, R. Spatio-temporal non-linear analysis of frog horizontal cells. Proc. U.S. - Japan Joint Seminar on Advanced Aanalytical Techniques Applied to the Vertebrate Visual System. (1979) pp.273-280

[71] Ogura, H. Orthogonal functionals of the Poisson process. IEEE Trans. on Information Theory (1972), IT-18, pp.473-481

[72] Piccolino, M. and Gershenfeld, H. H. Lateral interactions in the outer plexiform layer of turtle retinas after atropine block of horizontal cells. Nature (1977), 268, pp.259-261

[73] Schwartz, E. A. Electrical properties of the rod syncytium in the retina of the turtle. J. Physiol. (1976), 257, pp.379-406

[74] Schwartz, E. A. Responses of single rods in the retina of the turtle. J. Physiol. (1973), 232, pp.503-514

[75] Schwartz, E. A. Rod-rod interaction in the retina of the turtle. J. Physiol. (1975), 246, pp.617-638

[76] Simon, E. J. Two types of luminosity horizontal cells in the retina of the turtle. J. Physiol. (1973), 230, pp.199-211

[77] Stell, W. K. The structure and relationships of horizontal cells and photoreceptor-bipolar synaptic complexes in goldfish retina. Am. J. Anat. (1967), 121, pp.401

[78] Stell, W. K. The morphological organization of the vertebrate retina. Handbook of Sensory Physiology VII/2. Ed. M.G.F. Fuortes, Springer-Verlag, New York, 1972

[79] Stell, W. K. Functional polarization of horizontal cell dendrites in goldfish retina. Invest. Opthalm. (1976), 15, pp.895-908

[80] Thibos, L. N. and Werblin, F. S. The response properties of the steady antagonistic surround in the mudpuppy retina. J. Physiol. (1978), 278, pp.79-99

[81] Tomita, T. Electrical responses of single photoreceptors. Proceedings of the IEEE (1968), 56, pp.1015-1023

[82] Toyoda, J., Nosaki, H., and Tomita, T. Light-induced resistance changes in single photoreceptors of Necturus and Gecko. Vision Res. (1969), 9, pp.453-463

[83] Toyoda J. ,Hashimoto, H. ,Anno, H. and Tomita, T. The rod response in the frog as studied by intracellular recording. Vision Res. (1970) 10, pp.1093-1100

[84] Toyoda, J.-I. and Tonosaki, K. Studies on the mechanisms underlying horizontal-bipolar interaction in the carp retina. Sensory Processes (1978), 2, pp.359-365

[85] Trifonov, Yu. A. Study of synaptic transmission between photoreceptor and horizontal cells by means of electrical stimulation of the retina. Biophysica (1968), 13, pp.809-817

[86] Werblin, F. S. Control of retinal sensitivity II. Lateral interactions at the outer plexiform layer. J. Gen. Physiol. (1974), 63, pp.62-87

[87] Werblin, F. S. Anomalous rectification in horizontal cells. J. Physiol. (1975), 244, pp.639-657

[88] Werblin, F. S. Light, voltage, and time dependant components of the rod response. Sensory Processes (1978), 2, pp.306-315

[89] Werblin, F. S. Transmission along and between rods in tiger salamander retina. J. Physiol. (1978), 280, pp.449-470

[90] Werblin, F. S. Integrative pathways in local circuits between slow-potential cells in the retina. The Neurosciences: Fourth Study Program. Ed. F. O. Schmitt, MIT Press, Cambridge, Mass.,1979

[91] Werblin F. S. and Dowling, J. E. Organization of the retina of the mudpuppy Necturus maculosus. II. Intracellular recording. J Neurophysiol. (1969), 32,pp.339-355